UNITED STATES
DEPARTMENT OF THE INTERIOR
Geologocal Survey

DISPERSION IN NATURAL STREAMS

by

Richard G. Godfrey and Bernard J. Frederick

Prepared in cooperation with the
United States Atomic Engergy Commission

Open-file report

Washington, D. C.
1963

UNITED STATES
DEPARTMENT OF THE INTERIOR
Geologocal Survey

DISPERSION IN NATURAL STREAMS

by

Richard G. Godfrey and Bernard J. Frederick

Prepared in cooperation with the
United States Atomic Engergy Commission

Open-file report

Washington, D. C.
1963

CONTENTS

ILLISTRATIONS

TABLES

TABLES (continued)

Abstract

Eleven tests were conducted to study the dispersion patterns of a radiotracer in five natural stream channels and in one canal. The radiotracer was injected as a line source. The patterns of dispersion that were observed in these channels were compared with patterns predicted by the theoretical models for one-dimensional flow developed by Taylor and other investigators. Analysis of the relation between time and concentration of the tracer at several sections in each of the six reaches shows that the available theoretical models are not adequate to describe the dispersion patterns actually observed. Dispersion coefficients determined from the test data are from 2 to 30 times greater than those predicted by the theoretical models. It is apparent that a better understanding of the dispersal phenomenon is needed in order to predict dispersion patterns in natural streams.

Symbols

A	cross sectional area of stream
$\overline{A}$	mean effective cross sectional area in reach
a	radius of pipe
b	top width of stream
C	mean concentration of tracer
C_{max}	maximum concentration
d	mean depth in cross section
E	constant
F	difference in water surface elevation between injection point and point of observation
K	mean dispersion coefficient
l_1, l_2	Pearson distribution properties
M	total amount of dispersing material injected into the flow
M'	total amount of dispersing material observed by probe
Q	mean discharge
R	mean hydraulic radius
n	Manning roughness coefficient
S	Slope of water surface
T	temperature
t	time
$\overline{t}$	time from injection to passage of the centroid of dispersed material
$\overline{t}_p$	time from injection to passage of maximum concentration
V	mean velocity
$\overline{V}$	mean effective velocity in reach

Symbols (continued)

V_*	mean shear velocity in reach
v	local velocity
X	distance along the direction of flow
X_1	distance measured from an intermediate reference
y	height from channel bed
α_3	skew coefficient
η	denominator of the exponent of power law velocity distribution
σ_t	standard deviation of dispersion pattern in terms of time
σ_x	standard deviation in terms of distance

Introduction

Industrial and domestic wastes, both treated and untreated, are frequently added to the flow of streams. Because these same streams may constitute a major source of industrial and public water supply it is important to know how these wastes disperse and how they are diluted as they move downstream. Most of the wastes can be classified as soluble or miscible contaminants.

This report compares the dispersion pattern of a radiotracer as observed in five reaches of natural channels, and one reach of a large canal, with the dispersion pattern predicted from theoretical models developed by Taylor and other investigators.

The study was made by the U. S. Geological Survey in cooperation with the U. S. Atomic Energy Commission, Division of Reactor Development. This report presents the results of only one of a number of cooperative studies relating to the problem of nuclear wastes, however, the results presented herein are applicable not only to dispersal of atomic materials but also to the dispersal of any soluble stable material that may be introduced into a stream.

Theoretical Models

Several investigators have developed mathematical models to describe the turbulent dispersion process in pipes and open channels assuming rather idealized conditions including uniform flow. These conditions are rarely, if ever, encountered in natural streams. Consequently, the numerical values derived from the theoretical models are generally not applicable to natural streams. However, certain information from the models, both qualitative and quantitative, can be used as the basis for the analysis of field data.

The basic equation for turbulent diffusion under steady uniform flow may be written as

$$\frac{\partial C}{\partial t} + V \frac{\partial C}{\partial x} = K \frac{\partial^2 C}{\partial x^2} \qquad (1)$$

where C is the mean concentration

V is the mean velocity

K is the mean effective or bulk dispersion coefficient

t is time

x is the distance along the flow direction

This form of the modified Fickian equation is based on the assumption of a constant K which, according to Taylor (1954), occurs only after the diffusing material has travelled a considerable distance downstream from the point of injection. Introducing a coordinate system moving with V, thus a new variable, $x_1 = x - Vt$, the equation is reduced to

$$\frac{\partial C}{\partial t} = K \frac{\partial^2 C}{\partial x_1}$$

A solution of the above equation which satisfies the initial condition of the introduction of concentrated material at x = 0 when t = 0 is

$$C = Et^{-\frac{1}{2}} \exp \frac{-x_1^2}{4Kt}$$

The arbituary constant E can be evaluated from the total amount of material added, M, and the cross sectional area of the stream, A, yielding

$$C = \frac{M}{A\sqrt{2\pi}\sqrt{2Kt}} \exp \frac{-(x-Vt)^2}{4Kt} \qquad (2)$$

From (2) several observations can be made. The maximum concentration occurs at $x = V t$ and will decrease as t becomes large hence as x becomes large. Also the dispersion pattern is normally distributed with a mean of $x = Vt$, and a standard deviation of $\sigma = \sqrt{2Kt}$. Note that the solution predicts the pattern of dispersion for a given value of K which must be evaluated independently from theory or by experiments which yield a normal dispersion pattern. The theoretical evaluation of K has been attempted by Taylor (1954) for pipe flow and by Elder (1959), Parker (1961) and I. E. Thomas (written communication) for open channel flow.

Taylor assumed that the local dispersion coefficient is equal to the momemtum exchange coefficient (Reynold's analogy). He also assumed that the transfer coefficient in the longitudinal direction was equal to the transfer coefficient in the radial direction. Lastly, he assumed that the effect of local longitudinal turbulence was independent of the effect of the local transverse turbulence coupled with the local transverse velocity gradient. Using the empirical transverse velocity distribution of Stanton and Pannell (1914) and Nikuradse (1932), he summed the rate of material transfer across a plane moving with the mean velocity, V, and obtained

$$K = 10.1 \quad aV_* \tag{3}$$

where a is the radius of the pipe

V_* is the mean shear velocity

The effect of longitudinal turbulence contributes only about 0.5 percent to the value of K.

Subsequently Elder (1959) applied a similar analysis to the case of an open channel. He assumed a logarithmic velocity distribution and found

$$K = 5.93\ dV_* \tag{4}$$

where d is the depth of flow

Again the effect of longitudinal turbulence is small, contributing only about 1 percent to the value of K.

Thomas (written communication) used Taylor's method to analyze a free surface flow. He assumed a power law velocity distribution.

$$v = v_{max} \left(\frac{y}{d}\right)^{\frac{1}{\eta}}$$

where v is the local velocity in the x direction at y

He found K to have the following form

$$K = \frac{dV^3}{V_*}\ \Phi(\eta) + \frac{dV_*^2}{V}\ \Psi(\eta) \tag{5}$$

Thomas evaluated $\Phi(\eta)$ and $\Psi(\eta)$ for η equal to 6, 7, 8, 9 and 10. The last term in (5) is the component due to the longitudinal transfer and is small compared to the convective term. Equation (5) is markedly different in form from (3) and (4).

In all cases the velocity was described as solely a function of the distance from the bed, which is not the case in man-made waterways and most natural streams. Tracy and Lester (1961) found that the velocity distribution in the vertical is affected by the side walls for a distance about 3 times the depth away from the walls.

Because these investigators have shown that the effective dispersion coefficient is largely the result of the velocity gradient, the one-dimensional picture of a velocity distribution underevaluates the dispersion coefficient in all uniform channels except those having an extremely large width-depth ratio.

In evaluating their models each investigator conducted either laboratory or field tests. Taylor was remarkably successful in substantiating his results with laboratory tests in small pipes at velocities of 7 feet per second; the Reynolds number equalled $1.93\ (10)^4$. With lower velocities (4 feet per second) Taylor found that the concentration-time curve was not symmetrical but steeper on the rising limb as compared to the falling limb. He attributed this to the thicker laminar layer which retained a portion of the tracer for a longer period. In applying his model to the pipe-line data of Hull and Kent (1952), Taylor showed that the observed value of the dispersion coefficient was about twice the theoretical value. One other significant observation was the effect of curvature in a pipe. The observed dispersion coefficient for a coil where the radius of curvature was 96 times the radius of the pipe also was double the theoretical value. Thus the assumption of uniform flow is limiting because the magnitude of the dispersion coefficient readily reflects any slight departures from uniformity.

Elder's experiments in a channel with depths from 1 to 1.5 cm gave skewed distance - concentration curves. He attributed this skew to that portion of the tracer being carried near the wall in the viscous sublayer. In determining the dispersion coefficients from his tests Elder ignored the long tails and was able to check his theoretical results within 10 percent.

Thomas conducted a field study in the Chicago Sanitary and Ship Canal for verification of his theoretical model. The canal, 26 feet deep and 160 feet in width, has a uniform cross-section. The dispersion coefficients determined from the experimental data were about 12 times greater than those computed from his model. The experimental results were 5 times greater than those from Elder's model and twice those from Taylor's model. Again the time-concentration curves were skewed.

When the dispersion coefficient is determined experimentally, it is preferable to express it in a dimensionless form:

$$\frac{K}{RV_*} = B$$

Where B is a dimensionless constant

As for the magnitude of B, it is expected that the experimental data will yield higher values than obtained from theoretical considerations because of the horizontal velocity gradient and the horizontal turbulence component existent in the actual flow. As shown by Taylor and Elder, the viscous sublayer, which provides temporary storage of the tracer and the channel curvature tend to increase the value of B over the theoretical value.

It should be emphasized that the basic dispersion equation (1) and its solution (2) are derived under the assumption of uniform random dispersion. Unfortunately, such randomness is not present in open channel flow. It is possible that the mean longitudinal distribution of the added material will deviate from a normal pattern. Therefore, the dispersion used in this analysis is that defined by Einstein's (1905) equation

$$K = \frac{\sigma_x^2}{2t}$$

where σ_x^2 is the variance of the longitudinal spread.

Design of Experiments

Several previous dispersion experiments by Thomas (written communication), Parker (1958), Simpson and others (1958) have been conducted in natural channels or canals. In each case the tracer was released from a point source for a finite time period. Glover (1961) used a multiple point source in a braided stream to simulate a plane source.

An instantaneous plane source would be required in order to directly compare the experimental results with the theoretical models. Fortunately, vertical mixing occurs very rapidly according to Wagener (written communication). Thus, a line source was used to simulate a plane source. (In all cases the width-depth ratio was large.)

A broad range of conditions is necessary to evaluate the influence of channel geometry and flow characteristics.

Six reaches used in this study are given below:

Reach	Alignment	Discharge (cfs)	Total Length (ft)	Total Fall (ft)
Clinch River (above gage) near Clinchport, Va.	Straight	240	21,800	6.69
Clinch River (below gage) near Speer's Ferry, Va.	Straight	323 3,000 1,800	19,300	6.85 7.38 7.35
Copper Creek (above gage) near Gage City, Va.	Crooked	35.0	27,550	79.87
Copper Creek (below gage) near Gage City, Va.	Straight	54.3 300 48.0	13,550	17.62 17.34 17.60
Powell River near Sneedville, Tenn.	Crooked	140	20,450	6.39
Coachella Canal near Holtville, Calif.	Straight	900 950	18,000	2.01

These sites were selected in order that the effect of alignment could be evaluated by comparing the Clinch River results with those from the Powell and from the two reaches of Copper Creek. In multiple tests on the same reach the geometry would be unchanged for all practical purposes therefore, the effect of depth and discharge could be evaluated.

For each test reach, horizontal and vertical control was established and a topographic map of the low-water channel was prepared. A sketch of each of the study reaches is included in the Supplementary Data Section. Six representative cross sections were chosen in each reach. Where multiple tests were made in the same reach, great care was exercised to use the same sections.

The tracer was injected in a line source across the stream either by wading or from a boat. About 15 ml of the highly concentrated solution of $AuCl_3$, was diluted to a volume of 2 liters using water from the stream to minimize the difference in specific gravity between the tracer and the stream. Because of the health hazards, the injection was started several feet from one bank and stopped short of the opposite bank. This practice minimzed contamination of the banks by the injected solution. The injection was made at a uniform rate over a one minute period. The amount of activity used in each test was proportional to the discharge (about 2 curies per thousand cubic feet per second of discharge). The resulting concentrations of activity dropped rapidly to a level below that specified as the maximum permissible concentration in unrestricted areas (see Code of Federal Regulations, Title 10, Part 20, Paragraph 20.106 and Appendix B, Table II, Column 2), but were sufficiently high to be easily detected at all cross sections within the reach.

Selection of a Radiotracer

The principal advantages of radioisotopes as tracers are the ease of detection, the large span of concentration that can be observed, and the high order of resolution. The art of measuring radiation has progressed at an amazing rate during the last fifteen years.

In considering a particular tracer problem the choice of isotope is largely determined by the available detecting equipment. Measurement in situ is highly advantageous in many open-channel tracer problems because the detailed dispersal pattern is unknown. A program of grab sampling would yield adequate results only if the time-of-travel of the labeled water were accurately known for proper timing of sample collection at the several measuring sites. Thus commercially available equipment was adapted for in situ measurement in stream channels.

A gamma-emitting isotope is preferred in field studies because of the greater ease of detection. Gamma scintillation techniques are highly perfected and permit the sensing of activity from a larger body of water. The associated beta emissions are largely absorbed by the waterproof detector housing and the water itself.

Radiation health physics play an important role in the selection of a radiotracer. The maximum permissable concentration of isotopes as given in the National Bureau of Standards Handbook 69 (1959) and the half-life of the isotope were considered. Radionuclides which are retained by organisms for long periods were not considered for use.

The half-life of the isotope should be sufficiently short in order that the activity rapidly reduces to very low levels upon completion of the experimental program. A short half-life also permits additional testing in the same location within a reasonable time. However, the half-life must be sufficiently long to allow for transport of the isotope to the test site and completion of the experiment.

Because the isotope is to be injected into a stream, it must be in a water-soluble form. In addition, the amount sorbed by the bed material and the biota should be a minimum. The final considerations are availability and cost.

Iodine-131 has been used by Archibald (1949), Parker (1958), and Ellis et al (1958) in tracing surface waters. Hull (1958) used Gold-198 as a tracer in several streams with very high recovery rates.

The characteristics of the two isotopes are

	Iodine-131	Gold-198
Half-life	8.05 days	2.70 days
Principal gamma radiation	0.364 mev	0.411 mev
Maximum permissable concentration in drinking water	$2(10)^{-6}$ $\mu c/_{ml}$	$5(10)^{-5}$ $\mu c/_{ml}$
Cost per millicurie	$\sim$ \$0.30	$\sim$ \$0.06

Gold-198 was chosen because of the higher permissable concentrations, shorter half-life and substantially less cost.

Radiation Detection Equipment

The concentrations of activity in the stream were observed by a scintillation detector with a 1 in. x 1 in. sodium iodide thallium activated crystal. A commercially available unit used in the medical field was adapted for field use by transistorizing the preamplifier and using a 100-foot lead. The probe assembly (crystal, photomultiplier tube and preamplifer) were housed in a waterproof case. The entire unit is shown in figure 1.

Figure 1. -- Photograph of probe assembly.

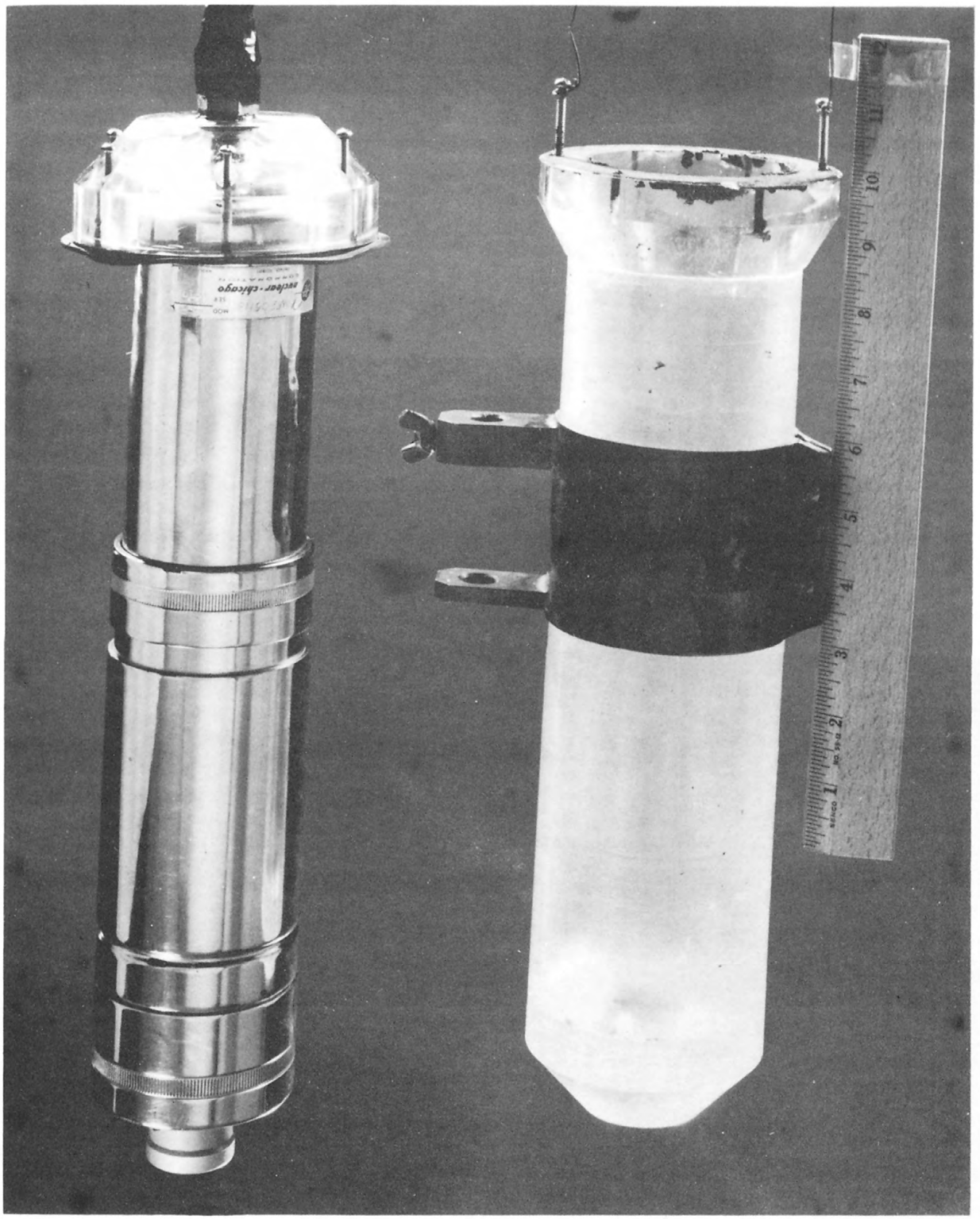

Figure 1. - Photograph of probe assembly

The probe was attached to a battery-operated five decade scaler shown in figure 2. The resolving time for the entire system was tested

Figure 2. -- Photograph of scaler.

by the two-source method (Price, 1958) and found to be 50 microseconds. The error due to the resolving time is about 5 percent at 60,000 counts per minute and 10 percent at 110,000 counts per minute.

The concentrations were measured at or near the centerline of the stream. Each cross section was provided with one set of equipment, a probe and scaler. The six sets of equipment were identical. In testing the relative counting rates versus the high voltage setting, minor differences were found in the optimum high voltage setting for each set. Thus each set was used and calibrated as a unit. In the end no sensible differences were found in the calibrations. However, probes and scalers were not interchanged without checking the calibration. Scalers were operated for a finite time period, 15, 30, 60 or 180 seconds, read and the observation recorded. The scaler was then reset and a new observation cycle was started at a predetermined time following a short pause for the recording of data.

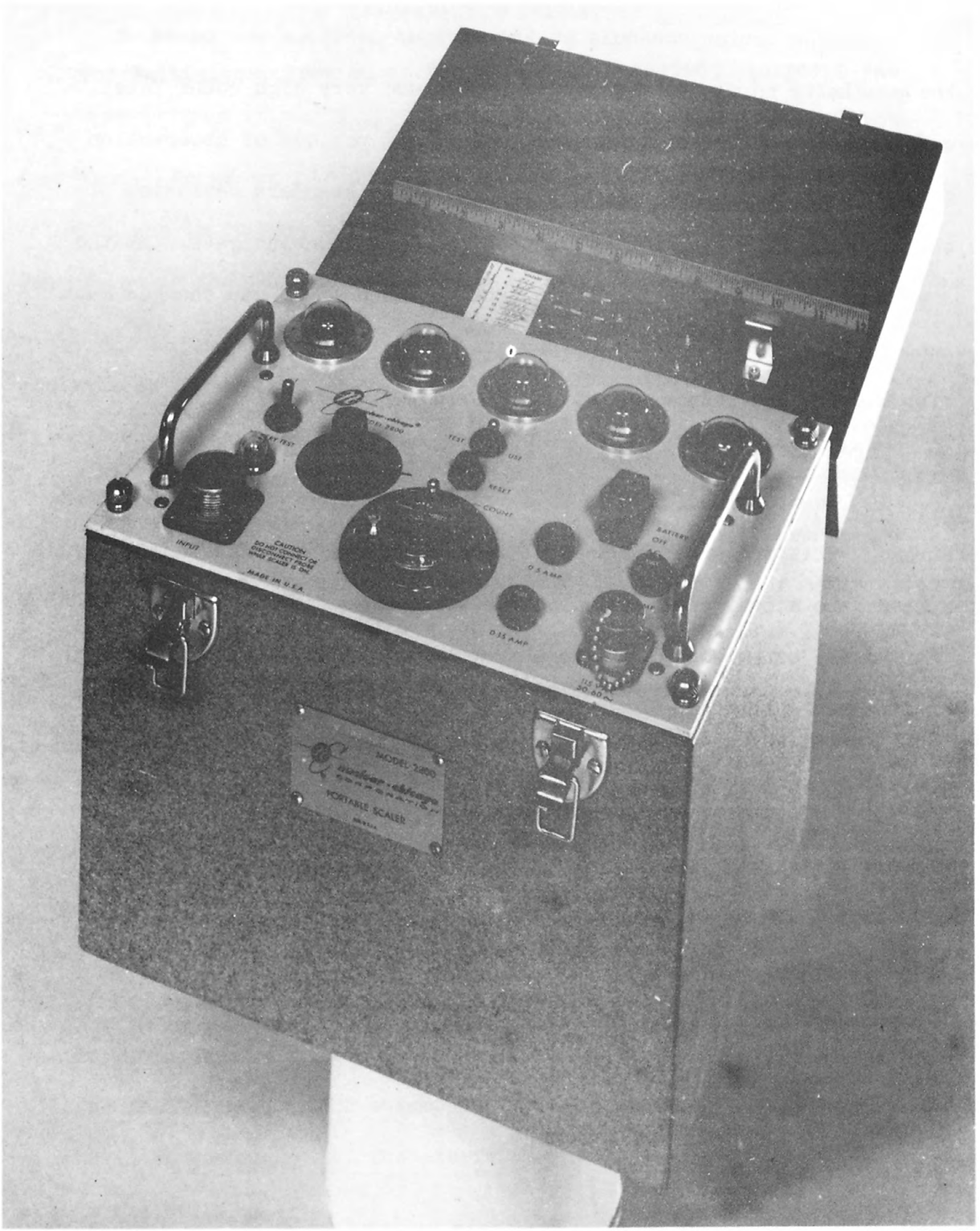

Figure 2. - Photograph of scaler

The observation schedule at the various sections was based on the proximity to the dosing section. Because very high count rates were obtained at the upstream sections, short periods of observation gave a sufficient number of counts to hold the standard deviation of the counting rate within 2 percent of the mean counting rate. At the downstream sections, the counting rate was much lower and changed much less rapidly. Longer counting periods were necessary to define the distribution and reduce the standard error.

Three methods were used to stabilize the probe in the stream.

1) The probe was clamped to a metal rod driven into the bed of the stream. This rod extended several feet above the water surface and was attached to a taut cable spanning the stream.

2) The probe was placed in a frame which in turn was clamped over an inflated automobile inner tube. The float was again stayed by a cable.

3) The probe was suspended from a boom extending over the prow of a small boat. The boat was fastened to a cable.

In all instances the probe was submerged at a predetermined distance below the water surface.

Calibration of Equipment

The initial calibration of the radiation detection equipment was made in a tank with a diameter of five feet and a water depth of about five feet. Known amounts of activity were placed in the tank and the solution was thoroughly mixed. The probe from each set of equipment was placed in the tank and lowered to a fixed depth. In the operating position the crystal was 6 inches below the water surface. The concentrations of activity were varied from 0.01 to 25.0 μc/cu ft. Background observations were taken for each probe in the operating position before any activity was added. Several samples of calibration mixtures were assayed at the National Bureau of Standards or Abbott Labaratories, Oak Ridge, and these assays were the basis for computation of activity in the calibration tank. The effect of the diameter and depth of the calibration tank on the calibration of the probes is sizeable (Frederick and Godfrey, 1961). To have "infinite" geometry with the detecting equipment used in this study, 3 to 4 feet of water labeled with Gold-198 would be needed in all directions from the crystal. Thus, the counting rate is very sensitive to the position of the crystal with respect to the water surface. Knowing the streams under study would have a range in depth at each section from about 1 to 10 feet as well as considerable variation in depth from section to section, absolute calibration for all the conditions was not attempted. Since relative concentrations were used in the analysis, the discrepancies in assays and geometry were obviated.

Presentation of Observations

The base data obtained in the eleven tests, are presented in the section entitled Supplementary Data. To facilitate the discussion of the tests they have been numbered and identified in Table 1.

Table 1. -- Identification of tests.

A typical set of time-concentration observations are shown in figure 3. In this test the depths were sufficiently great to minimize

Figure 3. -- Time-concentration curves for test 1-61.

the effect of variations in geometry from section to section. Notice the continual decrease in peak concentration and the increase in time from the rising to falling limb as the tracer moves downstream.

Table 1 - Identification of tests

Test Number	Location	Date
1-59	Copper Creek (below gage) near Gate City, Virginia	June 9, 1959
2-59	Clinch River (below gage) at Speers Ferry, Virginia	June 16, 1959
3-59	Copper Creek (above gage) near Gate City, Virginia	June 18, 1959
4-59	Powell River above Four Mile Creek near Sneedville, Tennessee	June 23, 1959
5-59	Clinch River above Clinchport, Virginia	June 25, 1959
1-60	Copper Creek (below gage) near Gate City, Virginia	January 14, 1960
2-60	Clinch River (below gage) at Speers Ferry, Virginia	February 9, 1960
3-60	Coachella Canal near Holtville, California	May 11, 1960
4-60	Coachella Canal near Holtville, California	May 12, 1960
1-61	Clinch River (below gage) at Speers Ferry, Virginia	July 12, 1960
2-61	Copper Creek (below gage) near Gate City, Virginia	July 14, 1960

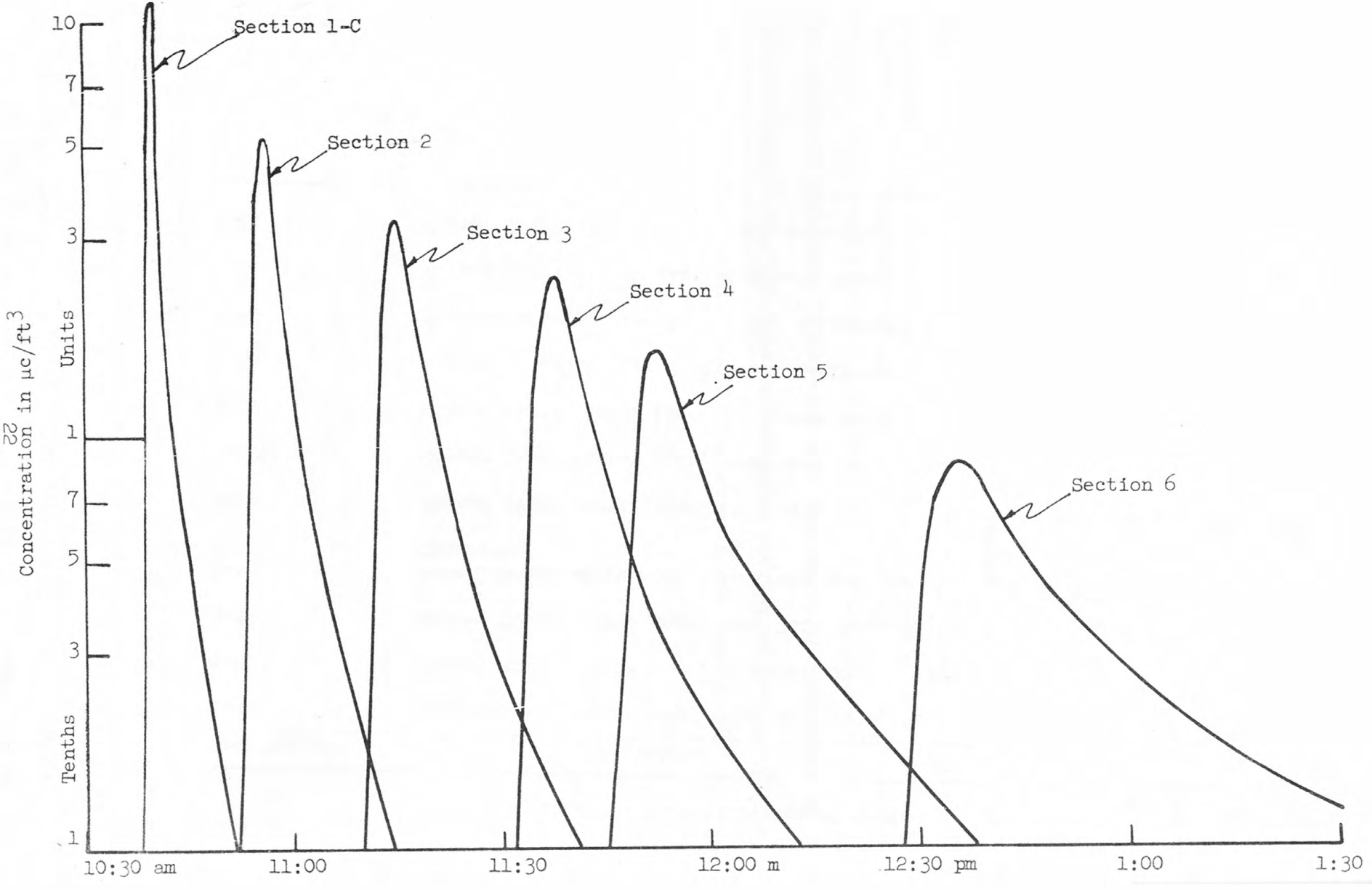
Section 1-C
Section 2
Section 3
Section 4
Section 5
Section 6
10
7
5
3
1
7
5
3
1
Units
Tenths
Concentration in μc/ft3
10:30 am
11:00
11:30
12:00 m
12:30 pm
1:00
1:30

Analysis

A number of parameters can be used to describe the pattern of dispersion in a natural stream. In view of the mathematical models developed earlier, the most significant parameter is the dispersion coefficient. Several methods of determining the mean or bulk dispersion coefficients were tried and will be discussed subsequently.

The method of moments was used to determine the mean time or the centroid of the time concentration distribution. This method was tried and rejected for the determination of the variance of each distribution. The influence of long and often inadequately defined tails gave very large values for the second moment.

A second method was to fit the data with a known statistical distribution which would follow the highly skewed data. The Pearson type III distribution has been successfully used to fit skewed hydrologic data and, after a preliminary study, this three-parameter distribution showed real promise in analyzing the observations. To obtain standard deviation and skew the following technique was used.

The ratio of l_2, the time from the maximum concentration along the falling limb, to l_1, the time along the rising limb to the maximum concentration was computed $(\frac{l_2}{l_1})$ for several levels of concentration.

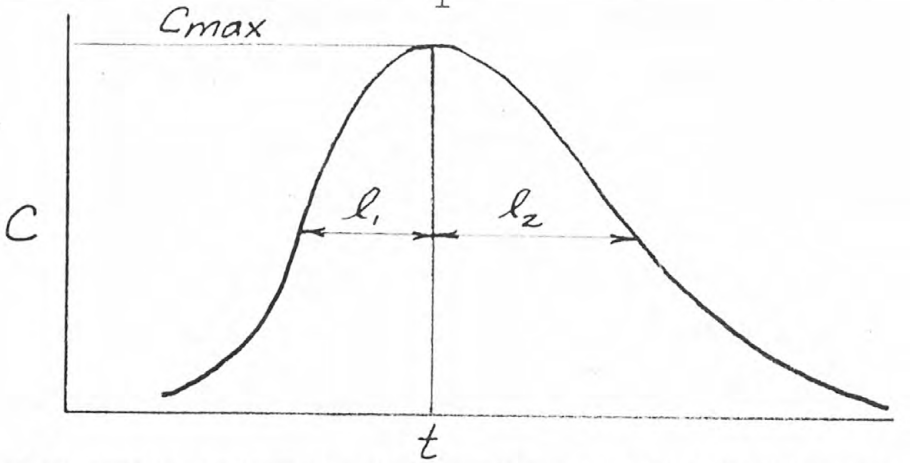

Table 2 determined from the Pearson Type III distribution was entered

Table 2. -- Properties of Pearson Type III distribution - theoretical values of l_2/l_1.

and an average value of skew was selected based on the l_2/l_1 ratios at concentration levels equal to 0.75, 0.61, 0.50, and 0.25 of the maximum concentration. Knowing the average skew α_3, for an observed distribution the lower segment of Table 3 was entered for this skew and the number

Table 3. -- Properties of Pearson Type III distribution - Number of standard deviation between rising and falling limbs.

of standard deviations between the rising limb and the falling limb was noted. Thus, knowing the time span at the several levels of concentration between the rising limb and the falling limb the standard deviation was readily determined. The mean standard deviation was obtained by averaging the values from the several levels of concentration.

Table 2 - Properties of Pearson Type III distribution

Theoretical values of $\frac{l_2}{l_1}$

C/C_{max} Skew (α_3)	0	.1	.2	.3	.4	.5	.6	.7	.8	.9
0.75	1.000	1.026	1.052	1.080	1.109	1.139	1.172	1.208	1.247	1.290
0.60653	1.000	1.034	1.069	1.106	1.146	1.188	1.233	1.283	1.338	1.399
0.50	1.000	1.040	1.082	1.126	1.174	1.225	1.280	1.341	1.408	1.485
0.25	1.000	1.057	1.118	1.183	1.254	1.332	1.418	1.514	1.622	1.748
0.10	1.000	1.074	1.155	1.242	1.339	1.446	1.567	1.705	1.864	2.051

	1.0	1.1	1.2	1.3	1.4	1.5	1.6	1.7	1.8	1.9
0.75	1.339	1.395	1.461	1.541	1.641	1.773	1.959	2.253	2.813	4.456
0.60653	1.469	1.551	1.648	1.767	1.919	2.124	2.420	2.901	3.849	6.686
0.50	1.573	1.676	1.799	1.953	2.154	2.422	2.821	3.476	4.788	8.689
0.25	1.985	2.072	2.290	2.567	2.936	3.451	4.228	5.533	8.128	15.649
0.10	2.275	2.549	2.893	3.339	3.941	4.794	6.084	8.223	12.413	24.562

Table 3 - Properties of Pearson Type III distribution

Number of Standard Deviations between Rising and Falling Limbs

C/C_{max} Skew (α_3)	0	.1	.2	.3	.4	.5	.6	.7	.8	.9
0.75	1.517	1.515	1.510	1.500	1.487	1.470	1.449	1.424	1.395	1.360
0.60653	2.000	1.998	1.990	1.979	1.962	1.940	1.913	1.881	1.843	1.800
0.50	2.355	2.352	2.344	2.330	2.311	2.286	2.255	2.218	2.174	2.124
0.25	3.330	3.327	3.316	3.298	3.273	3.241	3.201	3.153	3.097	3.032
0.10	4.292	4.288	4.276	4.256	4.228	4.191	4.146	4.093	4.030	3.958

	1.0	1.1	1.2	1.3	1.4	1.5	1.6	1.7	1.8	1.9
0.75	1.321	1.276	1.224	1.166	1.100	1.024	0.936	0.833	0.707	0.545
0.60653	1.748	1.690	1.625	1.551	1.467	1.371	1.260	1.131	0.977	0.786
0.50	2.066	2.000	1.925	1.840	1.744	1.636	1.511	1.367	1.198	0.944
0.25	2.959	2.875	2.781	2.675	2.557	2.425	2.277	2.112	1.925	1.708
0.10	3.877	3.786	3.684	3.572	3.449	3.314	3.168	3.008	2.832	2.623

Notice that the mean time, $\bar{t}$, and the standard deviation, σ_t, are determined soley by the shape of the distribution not by absolute value of the ordinates. Thus the effects of the varied geometry, errors in calibration and loss of isotope does not affect the computation.

Tables in the Supplementary Data section give all data used in the plotting of figures 4-13. In addition the time from injection to the maximum concentration, t_p, is shown. The difference between the elapsed time from injection to the mean time, $\bar{t}$, and the time of the peak, t_p, is another indication of skew. The shear, V_*, is shown as it will be used in the comparison of the field observations with the field observations with the theoretical models. Because of the non-uniformity in the reaches the shear velocity as computed from $\sqrt{gRS}$ cannot be considered a precise value as both the hydraulic radius and the slope vary from section to section.

The dispersion coefficient is

$$K = \frac{\sigma_x^2}{2\,\bar{t}}$$

the units of K as used herein are in feet squared per second. To get σ_x, the standard deviation in terms of feet, σ_t, is multiplied by the mean velocity $\bar{V}$ obtained from $\bar{t}$ and the distance from the dosing point, X, or

$$K = \frac{\sigma_t^2\, X^2}{2\bar{t}^{\,3}}$$

It is assumed that $\sigma_t\, \bar{V}$ equals σ_x. This assumption is only valid when values of ratio K/VX are small (Godfrey, 1961). In the final determination of K any distortion due to this assumption did not bias the analysis.

An alternate value of K can be computed by assuming that the time-concentration distribution is normal. It can be shown that

$$C_{max} = \frac{M}{A\sqrt{2\pi}\sqrt{2K\bar{t}}}$$

proveded x is sufficiently large and $\frac{K}{VX}$ is small.

Thus

$$K = \left(\frac{M}{C_{max}}\right)^2 \frac{1}{A^2\, 4\pi\bar{t}}$$

Since M is not accurately known and C_{max} is affected by the geometry of the measuring location, the ratio of $\frac{M^1}{C_{max}}$ is used. M^1 is the total amount of activity "seen" by the probe (to distinguish between the activity as assayed and the activity seen by the probe) and is directy related to the area under the time-concentration curve. Both M^1 and C_{max} are relative measures but the ratio is a true value.

In equation (2), A is an average area for the reach under consideration. This is computed from the known discharge (Q) which is constant through the reach and the mean velocity ($X/\bar{t} = V$)

$$\bar{A} = \frac{Q}{V}$$

Rather than computing K by the two methods for each section of the reach, an attempt was made to obtain a general or overall value of K for each test. The equations were converted to

$$\sigma_x = \sqrt{2K}\ \sqrt{\bar{t}}$$

and

$$\frac{M^1}{C_{max}\ \bar{A}\sqrt{2\pi}} = \sqrt{2K}\ \sqrt{\bar{t}}$$

The left-hand part of the above two equations are plotted as the ordinates against $\sqrt{\bar{t}}$ for each test. (Test 3-60 and 4-60 are shown on the same plot). The slope of the line is equal to $\sqrt{2K}$ and the resulting value of K is shown on figures 4-13.

Figure 4.	Dispersion Analysis	Test 1-59
Figure 4.	Dispersion Analysis	Test 2-59
Figure 6.	Dispersion Analysis	Test 3-59
Figure 7.	Dispersion Analysis	Test 4-59
Figure 8.	Dispersion Analysis	Test 4-59
Figure 9.	Dispersion Analysis	Test 1-60
Figure 10.	Dispersion Analysis	Test 2-60
Figure 11.	Dispersion Analysis	Test 3-60,4-60
Figure 12.	Dispersion Analysis	Test 1-61
Figure 13.	Dispersion Analysis	Test 2-61

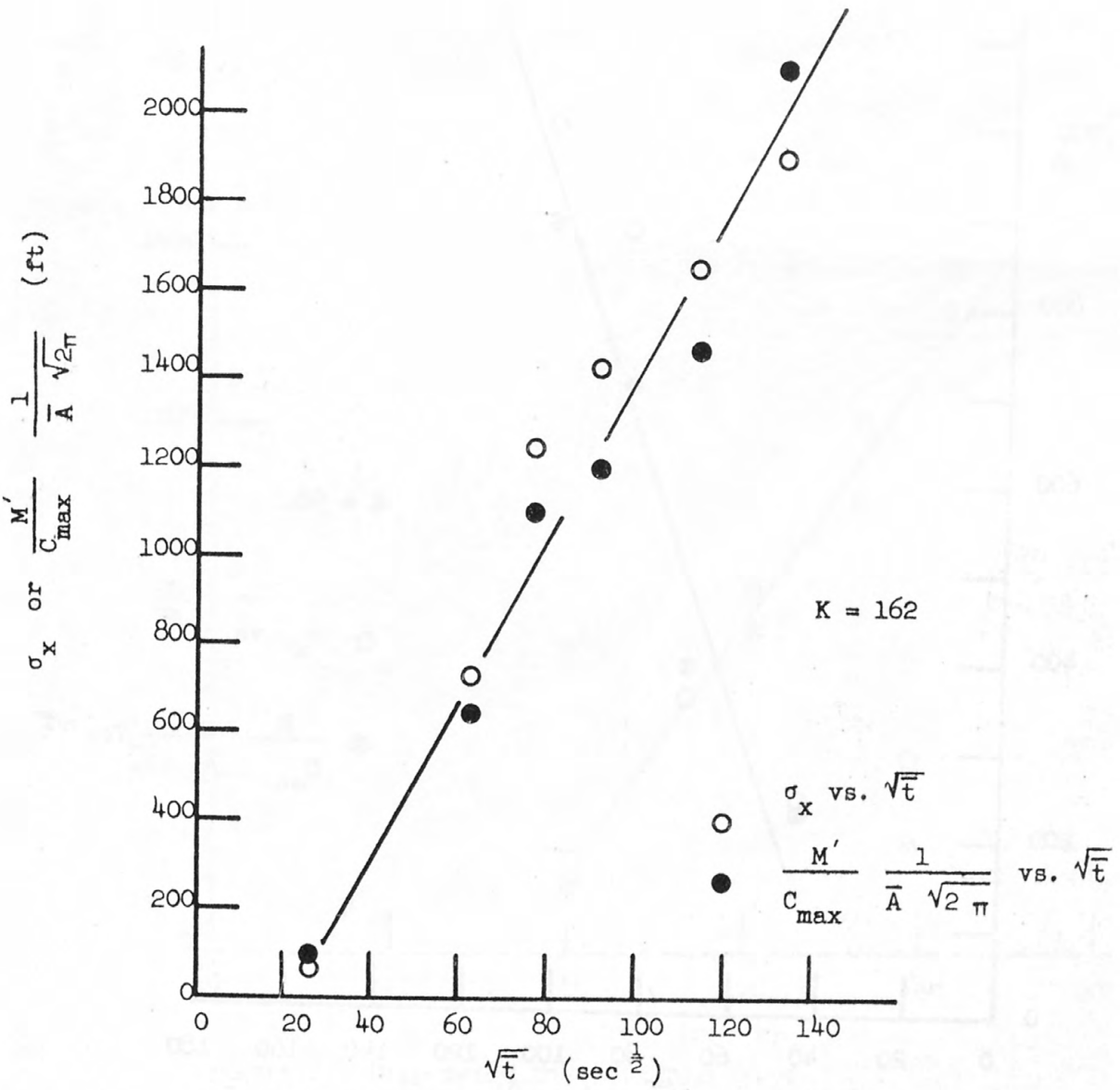

Figure 4. Dispersion Analysis Test 1-59

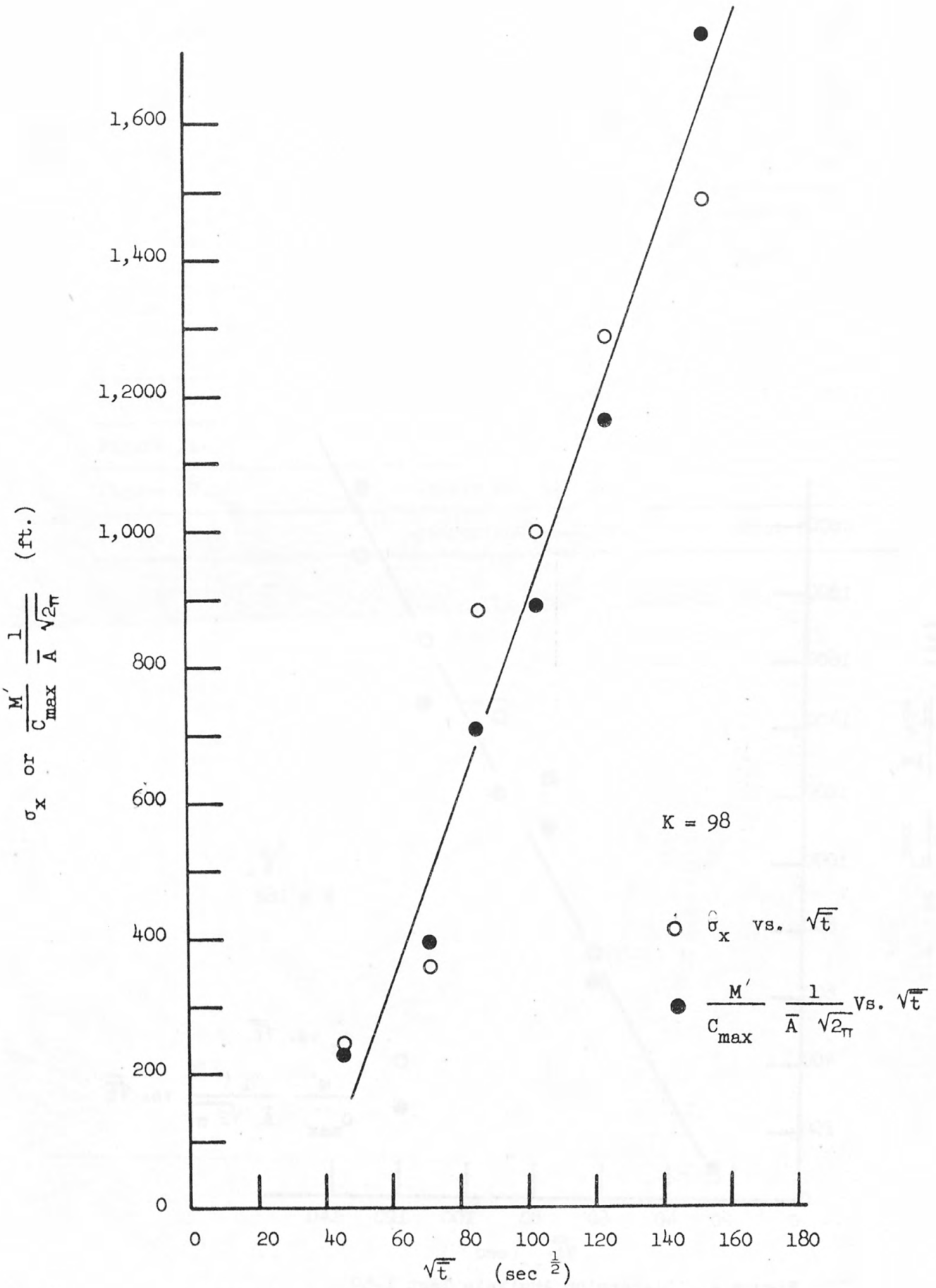

Figure 5. Dispersion Analysis Test 2-59

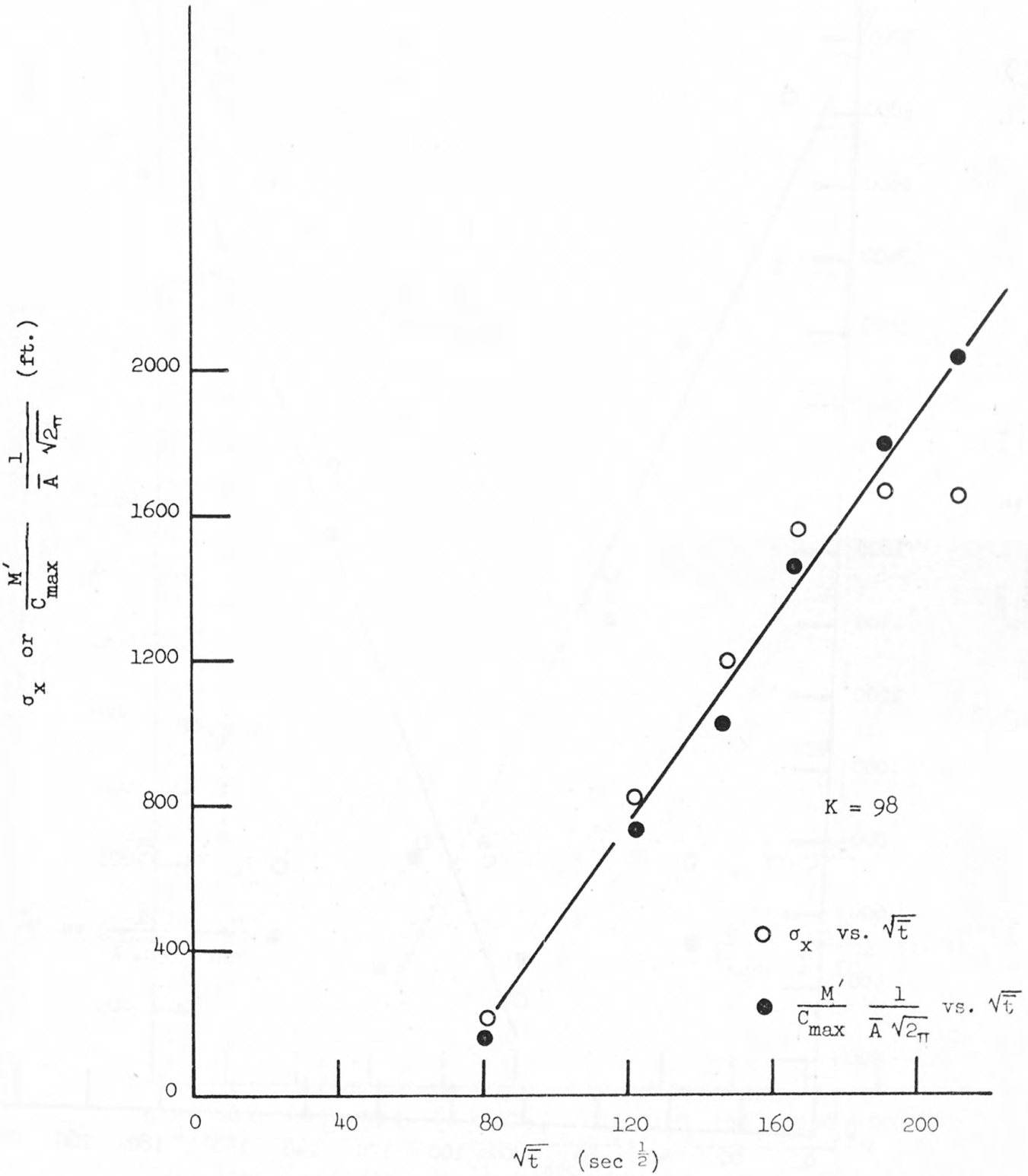

Figure 6. Dispersion Analysis Test 3-59

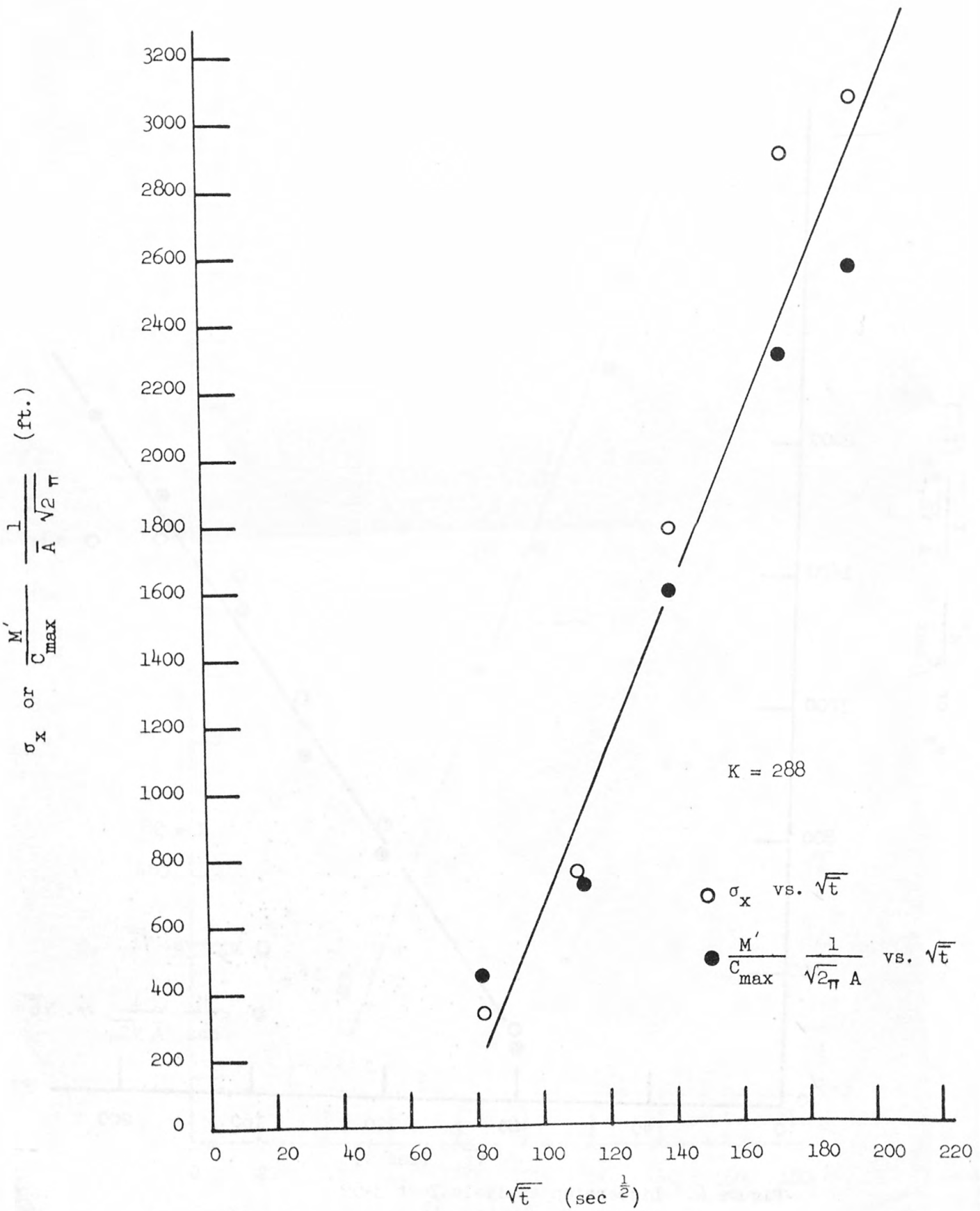

Figure 7. Dispersion Analysis Test 4-59

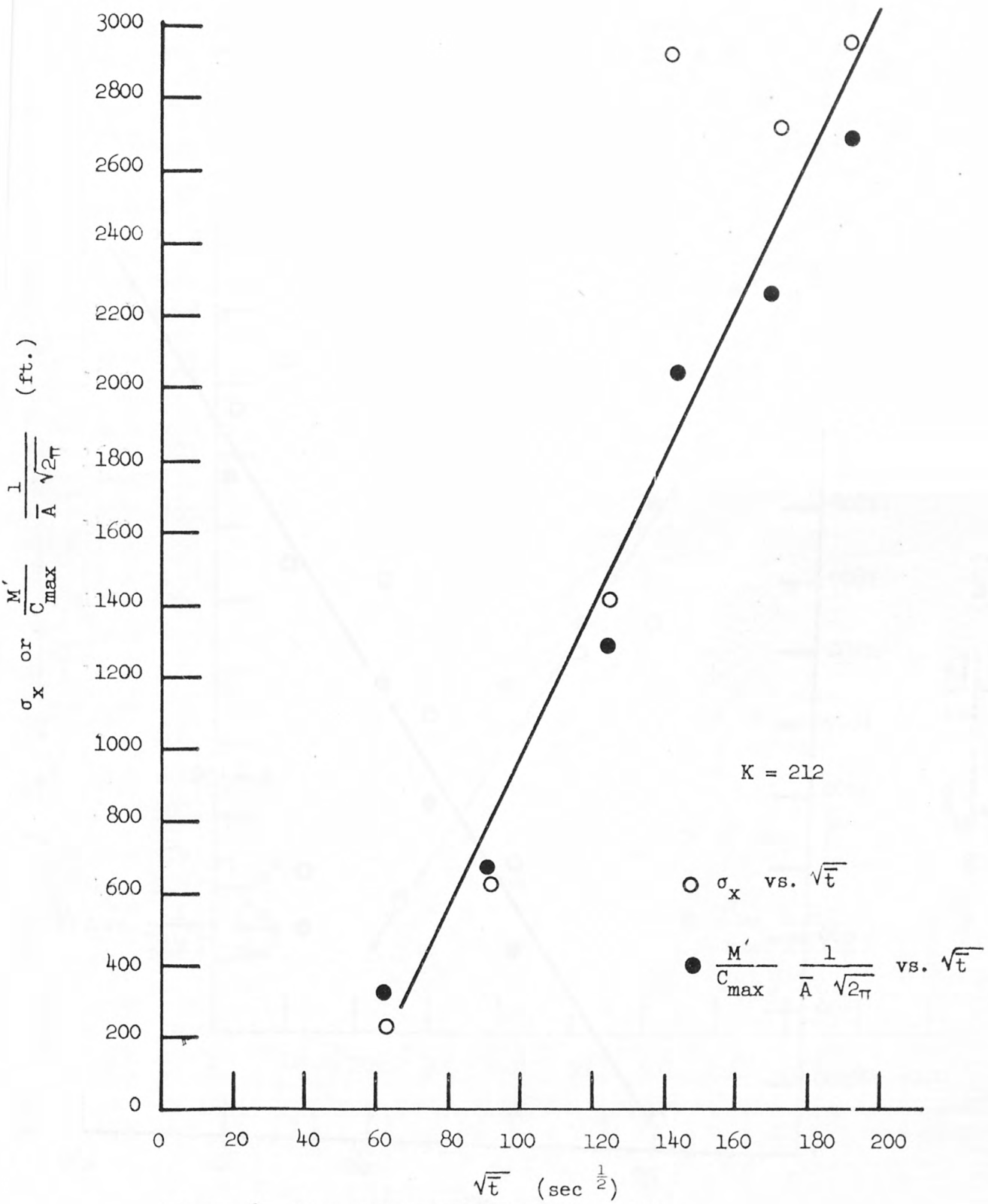

Figure 8. Dispersion Analysis Test 5-59

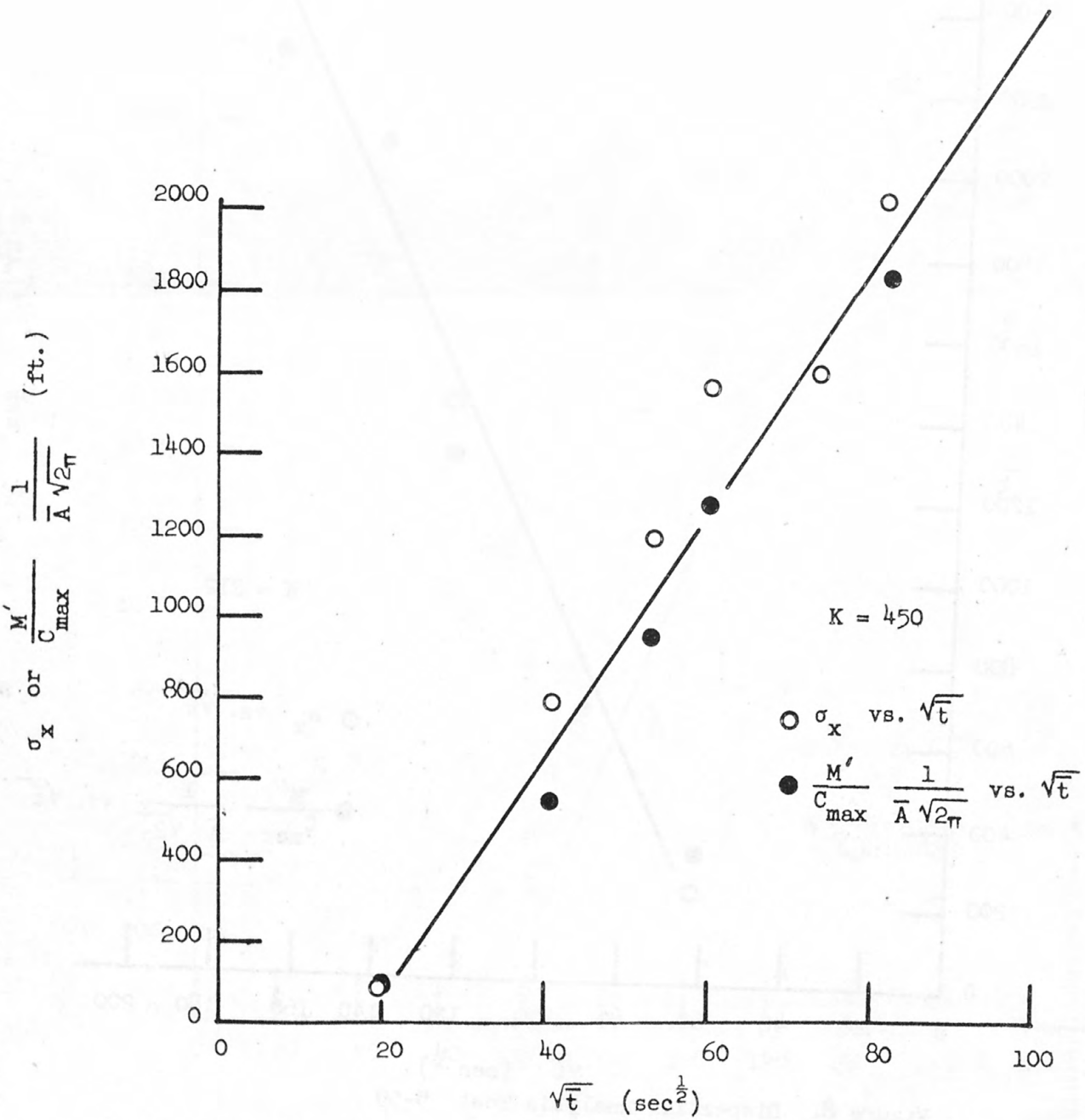

Figure 9. Dispersion Analysis Test 1-60

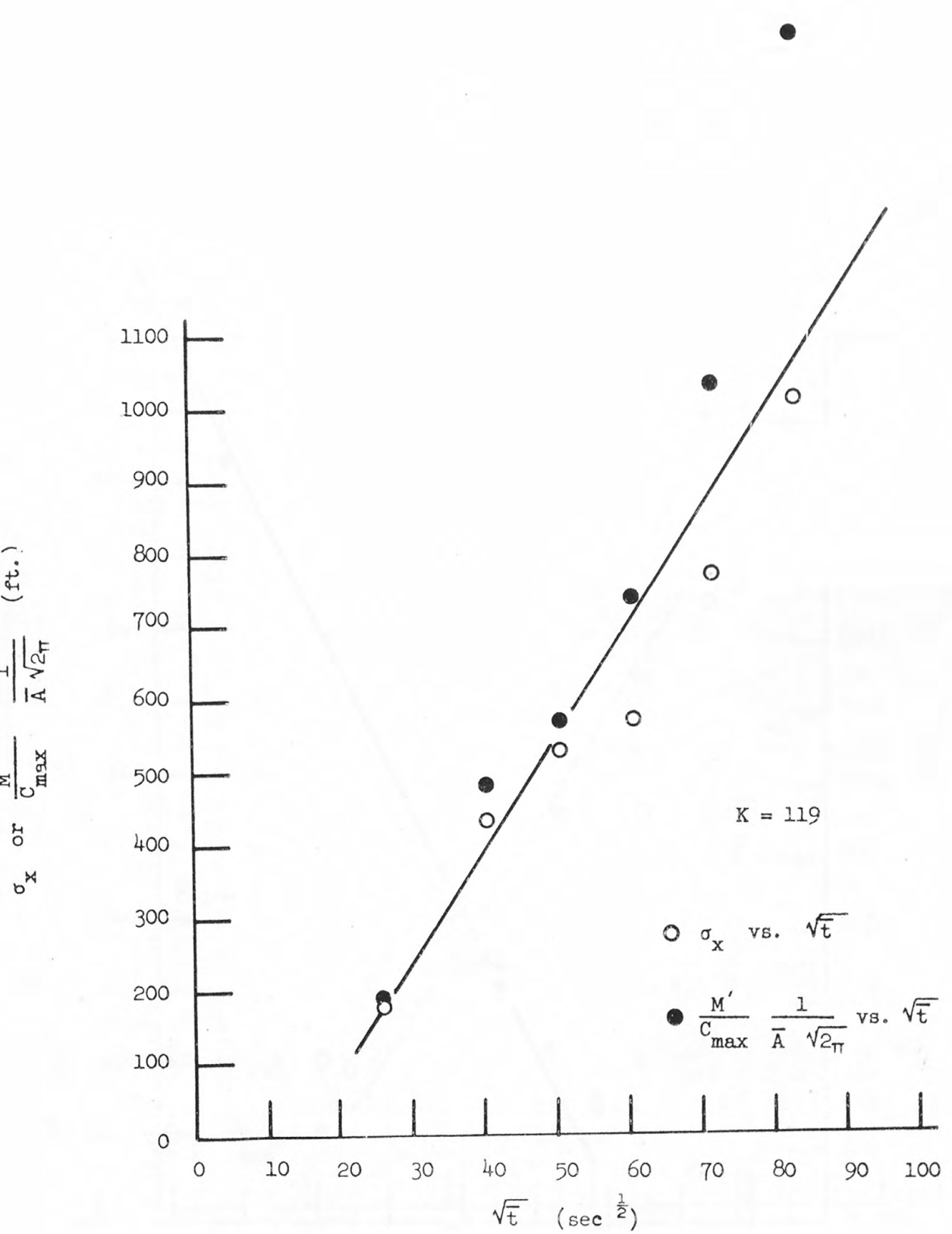

Figure 10. Dispersion Analysis Test 2-60

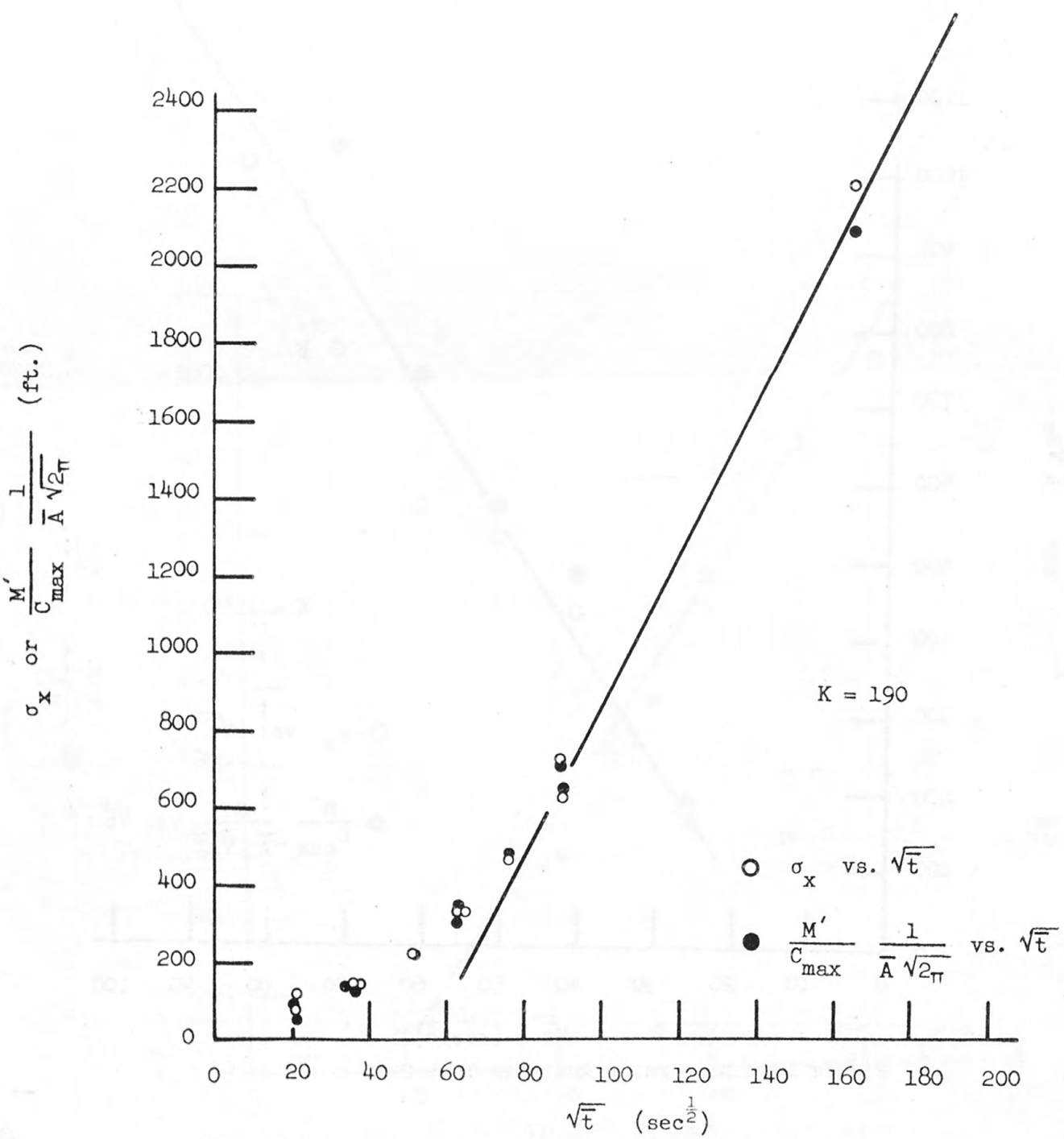

Figure 11. Dispersion Analysis Test 3-60, 4-60

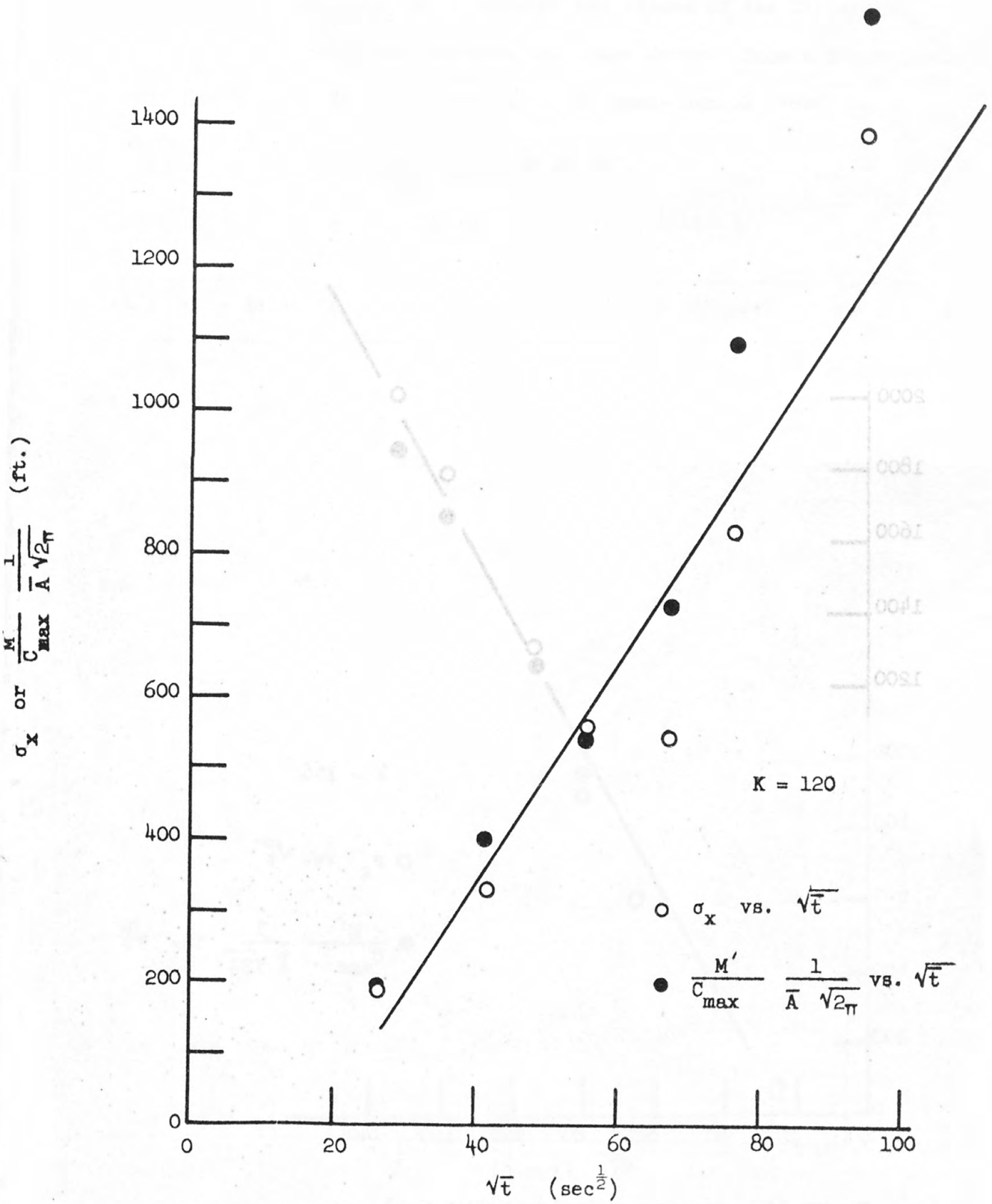

Figure 12. Dispersion Analysis Test 1-61

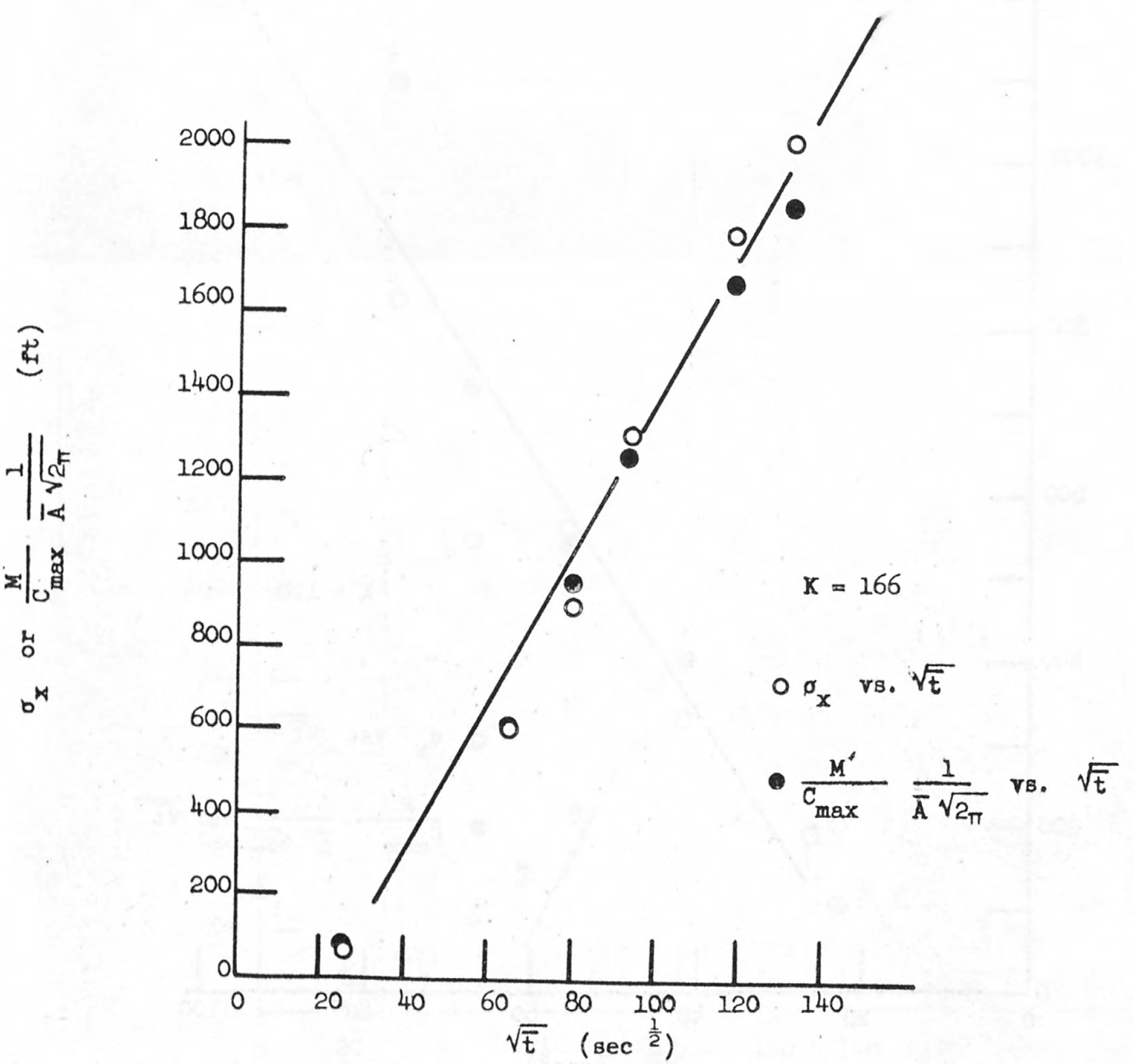

Figure 13, Dispersion Analysis Test 2-61

Lastly a comparison can be made of the values of the dispersion coefficients computed from the data and those derived from a theoretical model. Using Taylor's model adapted to the open-channel where

$$K_{theory} = 20.2RV_*$$

The relation of these coefficients is shown in table 4.

Table 4. - Relation of theoretical and observed dispersion coefficients

Table 4. - Relation of theoretical and observed dispersion coefficients

Test number	Discharge cfs	Bulk dispersion coefficient ft^2/sec K_{obs}	K_{theory}	$\frac{K_{obs}}{K_{theory}}$
Copper Creek (below gage) near Gate City, Virginia				
1-59	54.3	162	9.2	17.6
1-60	300	450	19.1	23.6
2-61	48.0	166	8.2	20.2
Clinch River (below gage) at Speer's Ferry, Virginia				
2-59	323	98	18.3	5.4
2-60	3000	119	47.3	2.5
1-61	1800	120	46.2	2.6
Copper Creek (above gage) near Gate City, Virginia				
3-59	35.0	98	9.2	10.7
Powell River above Four Mile Creek near Sneedville, Tennessee				
4-59	140	288	8.9	32.4
Clinch River above Clinchport, Virginia				
5-59	240	212	8.0	26.5
Coachella Canal near Holtville, California				
3-60	900	190	13.8	13.8
4-60	950			

Discussion of results

Analysis of all data shows some interesting features of turbulent dispersion in natural streams. One is the clear deviation from the normal distribution that is expected from the one-dimensional models. Another feature is the discrepancy between the dispersion coefficient obtained from the observations and that predicted from theoretical considerations.

In every test the skew coefficient, α_3, was between 0.5 and 1.7 with an overall average value between 1.1 and 1.2. Even though the technique for determining skew assumed a Pearson type III distribution and lacked precision, the consistently large values of skew obtained show that the one-dimensional models do not fit the field observations. There is no marked evidence that the skew decreases as the tracer cloud travels downstream. Thus as far as the field observations are concerned the normal distribution was not found even as an asymptote.

As previously mentioned, the velocity gradient in the transverse direction as well as the distortion of the vertical velocity curves near the banks tend to produce the skewed time-concentration curves. A second factor is the influence of non-uniformity in the reach. Comparison of the three tests on the lower Clinch show that the amount of skew decreases as discharge increases. At higher flows the effect of pools, riffles, expansions, and contractions are diminished and the skew coefficient is smaller. This effect can be seen to a lesser extent from the comparison of the Coachella Canal data with that for the natural streams. Unless the cause of skew is explained by a more appropriate theory, it seems that the empirical Pearson type III distribution describes the distribution pattern more accurately than the normal distribution.

The ratios of observed to theoretical value of K range from 2.5 to 32.4 as shown in Table 4 . There is a slight trend for better agreement in the more uniform straight reaches. Qualitatively such results are to be expected from theoretical considerations. However, magnitude of the discrepancies is surprising and discouraging.

In each plot, Figures 4-13, the line drawn through the data does not pass through the origin but intersects the abscissa some distance to the right of the origin. In the conduct of the tests a line source was used. The tracer was injected into the stream at a depth of about 6 inches. The injection was started a short distance from one bank and stopped a similar distance from the opposite bank. Thus, the steep velocity gradients near the banks and bed did not play their full role until the tracer cloud had migrated to the boundary. Even though an ideal plane source had been achieved, the tracer cloud would have had to travel a considerable distance before the dispersion process approached randomness. The combined effect of all of these limitations can best be seen in Figure 11 where the last observation crosssection was 63,750 feet downstream from the dosing point. The plotted points show an increasing rate of dispersion until the cloud had travelled several miles. Beyond this point the data can be described by the straight line shown on the figure indicating a constant value for the dispersion coefficient.

Lastly, consideration should be given to the use of such a model to compute the dispersion pattern of a contaminant. In equation (2) C_{max} is inversely proportional to $\sqrt{K}$. The standard deviation of the dispersed cloud is proportional to $\sqrt{K}$. Thus, even though it may not be possible to know K within 25 fold, the error in the maximum concentration and standard deviation is only 5 fold. Because the theory gives low values of K the predicted value of the maximum concentration would be too high and the predicted length of the cloud of dispersed material would be too short, in comparison with the field observations.

Supplementary Data

For each test the following data are presented. The time-concentration data are summarized for the sections available. All channel geometry and flow data are presented based on the discharge measurements and topographic information. Thirdly, the analysis data derived from the above information are given. These serve as the basis for dispersion analysis plots (figures 4-13).

TABLES

Table 5 -- Time-Concentration Data, Test 1-59

[Discharge: 54.3 cubic feet per second; Tracer: 0.067 curies of Au 198 1/; Time of injection: 11:21.0 to 11:22.0 a.m. EST]

Section 1 X = 630 ft		Section 2 X = 3,310 ft		Section 3 X = 5,670 ft	
Time	Concentration	Time	Concentration	Time	Concentration
11:27.5 a.m.	0	12:00.5 p.m.	0	12:26.0 p.m.	0
11:28.0	0.08	12:01.5	0.02	12:30.0	0.03
11:28.5	1.06	12:03.0	.13	12:37.0	.20
11:29.0	4.51	12:06.5	.38	12:42.0	.30
11:29.8	5.13	12:09.5	.52	12:46.0	.36
11:30.5	3.40	12:14.0	.59	12:50.0	.38
11:30.7	2.67	12:18.0	.54	12:53.0	.38
11:31.3	2.03	12:22.0	.47	12:57.0	.36
11:32.0	1.67	12:30.5	.33	1:10.0	.25
11:37.0	.55	12:36.5	.24	1:25.0	.04
11:41.7	.20	12:45.0	.16	1:39.0	.06
11:48.0	.04	12:49.0	.12	1:45.0	.04
11:55.5	0	1:03.0	.06	2:05.0	0
		1:17.0	.02		
		1:38.5	0		

Section 4 X = 7,870 ft		Section 5 X = 11,000 ft		Section 6 X = 13,550 ft	
12:54.0 p.m.	0	1:55.0 p.m.	0	2:28.0 p.m.	0
12:56.0	0.02	2:03.0	0.02	2:28.0 p.m.	0.02
1:00.0	.06	2:13.0	.08	2:58.0	.10
1:11.0	.22	2:21.0	.15	3:12.0	.17
1:16.0	.30	2:31.0	.21	3:34.0	.21
1:23.0	.34	2:36.0	.23	3:40.0	.21
1:25.0	.34	2:43.0	.25	4:04.0	.16
1:36.0	.29	2:51.0	.24	4:18.0	.13
1:44.0	.24	3:03.0	.21	4:38.0	.09
1:53.0	.18	3:18.0	.15	4:58.0	.06
2:03.0	.12	3:28.0	.12	5:28.0	.05
2:13.0	.08	3:43.0	.08	6:48.0	.02
2:26.0	.05	3:53.0	.06	8:08.0	0
2:41.0	.03	4:13.0	.03		
3:01.0	0	4:27.0	0		

1/ Concentrations are shown in micro-curies per cubic foot of Au 198.

Table 6 - Channel Geometry and Flow Data, Test 1-59

Section	1	2	3	4	5	6
X (ft)	630	3,310	5,670	7,870	11,000	13,550
Q (cfs)'	58.4	58.1	56.1	56.8	56.2	58.3
V (ft/sec)'	0.62	0.83	0.74	0.78	0.66	0.53
A (sq ft)'	95.1	70.2	76.0	72.4	84.9	110
b (ft)'	47	49	51	48	58	58
d (ft)'	2.02	1.43	1.49	1.51	1.46	1.90
R (ft)'	1.99	1.42	1.48	1.49	1.45	1.89
T (°F)	70	69	70	70	71	66
F (ft)	0.73	4.86	8.00	11.06	14.10	17.62
$S^{\frac{1}{2}}$	0.034	0.038	0.038	0.038	0.036	0.036
n	0.14	0.12	0.11	0.11	0.11	0.12

Based on discharge measurements made one day before tracer injection. Other data obtained from observations made during tracer test.

Table 7 Analysis Data, Test 1-59

[Q = 54.3; M = 0.067 curies]

Section	1	2	3	4	5	6
$\bar{X}$ (ft)	630	3,310	5,670	7,870	11,000	13,550
$\bar{t}$ (sec)	672	3,890	5,870	8,220	13,100	17,600
$\bar{V}$ (ft/sec)	0.938	0.851	0.966	0.960	0.840	0.770
$\bar{A}$ (sq ft)	57.9	63.8	56.2	56.6	64.6	70.5
σ_x (ft)	60.9	726	1,240	1,430	1,650	1,900
$\bar{t}\,\frac{1}{2}$ ($sec^{\frac{1}{2}}$)	25.9	62.4	76.6	90.7	114	133
α_3	1.1	1.3	1.2	1.3	1.1	0.8
M (curies)	0.065	0.060	0.059	0.058	0.059	0.078
M'/M	0.970	0.896	0.881	0.866	0.881	1.164
C_{max} ($\mu c/ft^3$)	5.13	0.59	0.38	0.34	0.25	0.21
t_p (sec)	510	3,180	5,400	7,380	12,100	15,300
$\frac{M'}{C_{max}\,\bar{A}\sqrt{2\pi}}$	87.6	638	1100	1200	1460	2100
V_* (ft/sec)	0.27	0.26	0.26	0.26	0.25	0.28

Table 8 -- Time-Concentration Data, Test 2-59

[Discharge: 323 cubic feet per second; Tracer: 0.744 curies of Au 198 1/; Time of injection : 11:29.5 to 11:30.5 a.m. EST]

Section 1 X = 2,260 ft		Section 2 X = 5,170 ft		Section 3 X = 8,170 ft	
Time	Concentration	Time	Concentration	Time	Concentration
11:52.0 a.m.	0	12:35.0 p.m.	0	1:10.0 p.m.	0
11:54.0	0.18	12:37.0	0.16	1:12.0	0.67
11:56.0	1.89	12:39.0	.60	1:15.0	1.15
11:57.0	3.20	12:41.0	1.38	1:17.0	1.45
11:58.0	4.03	12:42.5	2.02	1:18.0	1.48
11:59.0	3.73	12:45.0	2.48	1:22.0	1.40
12:01.0 p.m.	2.68	12:47.0	2.30	1:26.0	1.16
12:03.0	1.46	12:49.0	1.84	1:30.0	.91
12:05.0	.99	12:52.5	1.14	1:35.0	.65
12:09.0	.55	12:57.5	.67	1:40.0	.47
12:15.0	.28	1:02.5	.40	1:45.0	.34
12:30.0	.07	1:10.0	.24	1:50.0	.27
12:50.0	0	1:17.5	.14	2:00.0	.17
		1:30.0	.08	2:30.0	.05
		2:15.0	0	3:15.0	0

Section 4 X = 11,800 ft		Section 5 X = 15,300 ft		Section 6 X = 19,300 ft	
1:51.0 p.m.	0	2:59.0 p.m.	0	4:30.0 p.m.	0
1:54.0	0.02	3:02.0	0.06	4:39.0	0.03
1:57.0	.14	3:08.0	.26	4:48.0	.17
2:00.0	.39	3:14.0	.57	4:57.0	.34
2:03.0	.79	3:21.0	.70	5:07.0	.44
2:06.0	1.09	3:29.0	.64	5:12.0	.45
2:09.0	1.19	3:35.0	.52	5:19.0	.41
2:12.0	1.16	3:44.0	.39	5:31.0	.34
2:15.0	1.06	3:50.0	.31	5:45.0	.27
2:21.0	.79	3:59.0	.23	6:05.0	.19
2:27.0	.59	4:15.0	.15	6:19.0	.15
2:33.0	.42	4:34.0	.09	6:39.0	.11
2:39.0	.32	4:59.0	.05	7:04.0	.08
2:50.0	.21	5:29.0	.03	7:30.0	.06
3:00.0	.15	6:04.0	0	8:12.0	.04
3:14.0	.10			8:50.0	.02
3:35.0	0.05			10.20.0	0
4:17.0	0				

1/ Concentrations are shown in micro-curies per cubic foot of Au 198.

Table 9 Channel Geometry and Flow Data, Test 2-59

Section	1	2	3	4	5	6
X (ft)---------	2,260	5,170	8,170	11,800	15,300	19,300
Q (cfs) -------	381	348	334	371	374	345
V (ft/sec) ---	0.76	1.32	1.16	0.69	0.59	0.35
A (sq ft) ----	504	263	288	541	633	973
b (ft) -------	150	145	135	166	176	156
d (ft) -------	3.36	1.81	2.13	3.26	3.60	6.23
R (ft) -------	3.32	1.81	2.12	3.20	3.58	6.16
T (°F) --------	72	72	67	73	74	74
F_1(ft) --------	1.11	3.31	5.01	5.56	6.57	6.85
$S^{\frac{1}{2}}$ ----------	0.022	0.025	0.025	0.022	0.021	0.019
n ----------	0.11	0.08	0.07	0.08	0.10	0.12

Based on discharge measurements made one day before tracer injection. Other data obtained from observations made during tracer test.

Table 10 Analysis Data, Test 2-59

[Q = 323 cfs; M = 0.744 curies]

Section	1	2	3	4	5	6
$\overline{X}$ (ft) ---------	2,260	5,170	8,170	11,800	15,300	19,300
$\overline{t}$ (sec)---------	2,000	5,020	7,380	10,600	15,400	23,300
$\overline{V}$ (ft/sec)------	1.13	1.03	1.11	1.11	0.994	0.828
$\overline{A}$ (sq ft)-------	286	314	291	291	325	390
σ_x (ft)---------	241	359	886	994	1,290	1,490
$\overline{t}^{\frac{1}{2}}$($sec^{\frac{1}{2}}$)------	44.7	70.9	85.9	103	124	153
α_3 ----------	1.5	1.2	1.6	1.5	1.5	1.1
M′(curies)------	0.663	0.772	0.763	0.774	0.664	0.759
M′/M ----------	0.891	1.038	1.026	1.040	0.892	1.020
C_{max} ($\mu c/ft^3$)---	4.03	2.48	1.48	1.19	0.70	0.45
t_p (sec)--------	1,710	4,530	6,510	9,570	13,900	20,600
$\frac{M'}{C_{max}\ \overline{A}\ \sqrt{2\pi}}$ --	230	395	708	892	1160	1730
V_* (ft/sec) ----	0.23	0.19	0.21	0.22	0.23	0.27

Table 11 -- Time-Concentration Data, Test 3-59

[Discharge: 35.0 cubic feet per second; Tracer: 0.064 curies of Au 198 1/; Time of injection: 9:49.5 to 9:50.5 a.m. EST]

Section 1 X = 2,350 ft		Section 2 X = 7,100 ft		Section 3 S = 11,000 ft	
Time	Concentration	Time	Concentration	Time	Concentration
11:23.0 a.m.	0	1:03.5 p.m.	0	2:41.5 p.m.	0
11:25.0	0.08	1:09.5	0.05	2:45.5	0.01
11:26.0	.19	1:15.5	.12	2:55.5	.05
11:29.0	.78	1:20.5	.19	3:05.5	.12
11:31.0	1.13	1:27.5	.30	3:15.5	.17
11:32.0	1.23	1:35.5	.37	3:20.5	.20
11:34.5	1.32	1:40.5	.38	3:25.5	.21
11:37.0	1.23	1:45.5	.37	3:30.5	.22
11:51.0	.42	1:55.5	.32	3:35.5	.22
11:55.0	.29	2:15.5	.20	3:40.5	.22
12:00.0 m	.19	2:35.5	.10	3:50.5	.20
12:06.0 p.m.	.10	2:50.5	.06	4:35.5	.08
12:13.0	.04	3:20.5	.02	4:45.5	.06
12:26.0	0	4:05.5	0	5:00.5	.04
				5:45.5	0

Section 4 X = 15,750 ft		Section 5 X = 21,250 ft		Section 6 X = 27,550 ft	
4:04.5 p.m.	0	5:30.0 p.m.	0	8:00.0 p.m.	0
4:30.5	0.10	6:00.0	0.02	8:30.0	0.01
4:50.5	.18	6:30.0	.05	9:00.0	.04
5:00.5	.20	7:00.0	.10	9:30.0	.08
5:08.5	.20	7:20.0	.14	9:45.0	.09
5:16.5	.20	7:35.0	.16	9:55.0	.10
5:30.5	.18	7:50.0	.15	10:05.0	.10
5:50.5	.13	8:10.0	.12	10:20.0	.08
6:10.5	.09	8:30.0	.09	10:40.0	.06
6:30.5	.06	9:00.0	.06	11:00.0	.05
6:40.5	.05	9:30.0	.04	11:30.0	.04
6:50.5	.04	10:00.0	.02	12:00.0	.02
7:10.5	.03	10:30.0	.01	1:30.0 a.m.	.01
7:50.5	.01	11:10.0	0	3:30.0	0
8:30.5	0				

1/ Concentrations are shown in micro-curies per cubic foot of Au 198.

Table 12 Channel Geometry and Flow Data, Test 3-59

Section	1	2	3	4	5	6
X (ft)	2,350	7,100	11,000	15,750	21,250	27,550
Q (cfs)[1]	36.2	34.0	34.3	32.2	38.2	40.9
V (ft/sec)[1]	0.85	0.37	0.50	0.40	0.53	0.53
A (sq ft)[1]	42.7	90.8	67.0	81.1	72.7	76.5
b (ft)[1]	31	66	66	61	58	55
d (ft)[1]	1.38	1.38	1.02	1.33	1.25	1.39
R (ft)[1]	1.36	1.32	0.99	1.32	1.21	1.38
T (°F)	66	67	70	71	70	70
F (ft)	11.02	31.35	44.22	52.21	65.24	79.87
$S^{\frac{1}{2}}$	0.068	0.067	0.063	0.058	0.055	0.054
n	0.15	0.23	0.21	0.22	0.21	0.21

[1] Based on discharge measurements made one day before tracer injection. Other data obtained from observations made during tracer test.

Table 13 Analysis Data, Test 3-59

Q = 35.0 cfs; M = 0.064 curies

Section	1	2	3	4	5	6
$\overline{X}$ (ft)	2,350	7,100	11,000	15,750	21,250	27,550
$\overline{t}$ (sec)	6,660	14,900	21,600	27,800	36,300	44,900
$\overline{V}$ (ft/sec)	0.353	0.477	0.509	0.567	0.585	0.614
$\overline{A}$ (sq ft)	99.2	73.4	68.8	61.7	59.8	57.0
σ_x (ft)	207	827	1,190	1,560	1,650	1,650
$\overline{t}^{\frac{1}{2}}$ ($sec^{\frac{1}{2}}$)	81.0	122	147	167	191	212
α_3	1.3	1.2	1.1	1.0	0.8	0.6
M′ (curies)	0.057	0.051	0.039	0.045	0.043	0.029
M′/M	0.891	0.797	0.609	0.703	0.672	0.453
C_{max} ($\mu c/ft^3$)	1.32	0.38	0.22	0.20	0.16	0.10
t_p (sec)	6,300	13,900	20,800	26,300	35,000	44,100
$\frac{M'}{C_{max}} \frac{1}{\overline{A}\sqrt{2\pi}}$	173	728	1,030	1,450	1,790	2,030
V (ft/sec)	0.45	0.44	0.36	0.38	0.34	0.36

Table 14 -- Time-Concentration Data, Test 4-59

[Discharge: 140 cubic feet per second Tracer: 0.260 curies of Au 198 1/; Time of injection: 8:49.0 to 8:50.0 a.m. EST]

Section 1 X = 3,150 ft		Section 2 X = 5,510 ft		Section 3 X = 11,000 ft	
Time	Concentration	Time	Concentration	Time	Concentration
10:03.0 a.m.	0	11:20.0 a.m.	0	12:48.0 p.m.	0
10:06.0	0.09	11:26.0	0.12	12:58.0	0.05
10:09.0	.41	11:32.0	.32	1:10.0	.14
10:12.0	.59	11:38.0	.44	1:22.0	.18
10:14.0	.63	11:42.0	.46	1:32.0	.19
10:16.0	.64	11:44.0	.46	1:42.0	.20
10:18.0	.63	11:46.0	.46	1:52.0	.19
10:20.0	.57	11:52.0	.42	2:10.0	.17
10:25.0	.45	12:00.0 m.	.37	2:30.0	.14
10:30.0	.37	12:20.0 p.m.	.24	3:00.0	.10
10:40.0	.27	12:40.0	.16	3:30.0	.06
11:00.0	.16	1:00.0	.11	4:00.0	.03
11:30.0	.08	1:30.0	.06	4:30.0	.01
12:10.0 p.m.	.02	2:10.0	.03	5:10.0	0
1:00.0	0	3:00.0	0		

Section 4 X = 15,750 ft		Section 5 X = 20,450 ft		Section 6 X = 23,600 ft
2:52.0 p.m.	0	4:40.0 p.m.	0	
3:25.0	0.08	5:10.0	0.02	
4:00.0	.15	5:40.0	.07	
4:15.0	.16	6:10.0	.10	
4:22.0	.16	6:30.0	.11	
4:30.0	.16	6:40.0	.11	Not Observed
4:45.0	.15	6:45.0	.11	
5:15.0	.13	6:50.0	.11	
6:00.0	.09	7:00.0	.11	
6:45.0	.06	7:40.0	.09	
7:30.0	.04	8:40.0	.05	
8:15.0	.02	9:40.0	.03	
9:00.0	.01	10:50.0	.01	
10:00.0	0	12:00.0	0	

1/ Concentrations are shown in micro-curies per cubic foot of Au 198.

Table 15 Channel Geometry and Flow Data, Test 4-59

Section	1	2	3	4	5	6
X (ft)	3,150	5,510	11,000	15,750	20,450	23,600
Q (cfs)[1]	146	161	148	137	140	145
V (ft/sec)[1]	0.38	0.99	0.48	0.31	0.49	0.50
A (sq ft)[1]	385	162	315	435	283	292
b (ft)[1]	103	100	118	122	122	101
d (ft)[1]	3.74	1.62	2.67	3.57	2.32	2.89
R (ft)[1]	3.69	1.61	2.64	3.55	2.30	2.87
T (°F)	67	74	74	76	76	-
F (ft)	1.39	2.37	3.83	4.60	6.39	-
$S^{\frac{1}{2}}$	0.021	0.021	0.019	0.017	0.018	-
n	0.20	0.13	0.12	0.14	0.13	-

[1] Based on discharge measurements made one day before tracer injection. Other data obtained from observations made during tracer test.

Table 16 Analysis Data, Test 4-59

Q = 140 cfs; M = 0.260 curies

Section	1	2	3	4	5	6
$\bar{X}$ (ft)	3,150	5,510	11,000	15,750	20,450	23,600
$\bar{t}$ (sec)	6,720	12,500	19,500	30,400	38,000	
$\bar{V}$ (ft/sec)	0.469	0.441	0.564	0.518	0.538	
$\bar{A}$ (sq ft)	299	317	248	270	260	
σ_{x_1} (ft)	334	760	1,770	2,890	3,060	
$\bar{t}^{\frac{1}{2}}$ ($sec^{\frac{1}{2}}$)	82.0	112	140	174	195	
α_3	1.1	1.4	1.4	1.4	1.2	
M′ (curies)	0.215	0.263	0.198	0.248	0.184	
M′/M	0.827	1.01	0.762	0.954	0.708	
C_{max} ($\mu c/ft^3$)	0.64	0.46	0.20	0.16	0.11	
t_p (sec)	5,220	10,500	17,600	27,200	35,500	
$\frac{M'}{C_{max}\,\bar{A}\sqrt{2\pi}}$	449	719	1,590	2,290	2,560	
V_* (ft/sec)	0.23	0.15	0.17	0.18	0.16	

Table 17 -- Time-Concentration Data, Test 5-59

[Discharge: 240 cubic feet per second Tracer: 0.377 curies of Au 198 1/; Time of injection: 9:09.5 a.m. to 9:10.5 a.m. EST]

Section 1 X = 3,000 ft		Section 2 X = 6,100 ft		Section 3 X = 11,000 ft	
Time	Concentration	Time	Concentration	Time	Concentration
9:55.0 a.m.	0	10:54.0 a.m.	0	12:19.0 p.m.	0
9:58.0	0.14	10:56.0	0.02	12:24.0	0.04
10:01.0	.76	10:59.0	.14	12:34.0	.17
10:04.0	1.25	11:02.0	.29	12:44.0	.29
10:05.5	1.34	11:05.0	.44	12:49.0	.31
10:07.0	1.24	11:08.0	.53	12:54.0	.29
10:10.0	.89	11:10.0	.55	1:05.0	.25
10:15.0	.51	11:12.0	.54	1:20.0	.19
10:20.0	.34	11:16.0	.46	1:40.0	.13
10:30.0	.19	11:20.0	.39	2:10.0	.08
10:40.0	.11	11:30.0	.27	2:50.0	.04
11:00.0	.04	12:00.0 m.	.10	3:40.0	.02
11:30.0	0	12:40.0 p.m.	.02	4:30.0	0
		1:20.0	0		

Section 4 X = 14,700 ft		Section 5 X = 18,400 ft		Section 6 X = 21,800 ft	
1:18.0 p.m.	0	3:18.0 p.m.	0	4:54.0 p.m.	0
1:25.0	0.03	3:42.0	0.05	5:04.0	0.02
1:32.0	.07	4:06.0	.10	5:20.0	.04
1:40.0	.12	4:30.0	.13	5:40.0	.07
1:50.0	.16	4:42.0	.13	6:00.0	.09
1:57.0	.18	4:54.0	.13	6:20.0	.10
2:01.0	.18	5:18.0	.11	6:30.0	.10
2:05.0	.18	5:42.0	.09	6:40.0	.10
2:15.0	.17	6:06.0	.07	7:00.0	.09
2:35.0	.15	6:30.0	.05	7:30.0	.07
2:55.0	.12	7:00.0	.03	8:15.0	.05
3:30.0	.08	7:40.0	.02	9:00.0	.03
4:30.0	.04	8:20.0	.01	10:30.0	.01
5:30.0	0	9:40.0	0	1:50.0 a.m.	0

1/ Concentrations are shown in micro-curies per cubic foot of Au 198.

Table 18 Channel Geometry and Flow Data, Test 5-59

Section	1	2	3	4	5	6
X (ft)	3,000	6,100	11,000	14,700	18,400	21,800
Q (cfs)[1]	205	216	210	202	179	208
V (ft/sec)[1]	1.00	0.72	1.58	1.24	0.64	0.76
A (sq ft)[1]	204	298	133	162	280	272
b (ft)[1]	126	141	88	84	110	156
d (ft)[1]	1.62	2.11	1.51	1.93	2.55	1.74
R (ft)[1]	1.62	2.11	1.51	1.91	2.53	1.70
T (°F)	77	75	77	76	77	77
F (ft)	1.81	2.10	4.87	5.84	6.13	6.69
$S^{\frac{1}{2}}$	0.025	0.019	0.021	0.020	0.018	0.018
n	0.04	0.05	0.04	0.04	0.04	0.04

[1] Based on discharge measurements made one day before tracer injection. Other data obtained from observations made during tracer test.

Table 19 Analysis Data, Test 5-59

Q = 240 cfs; M = 0.377 curies

Section	1	2	3	4	5	6
$\overline{X}$ (ft)	3,000	6,100	11,000	14,700	18,400	21,800
$\overline{t}$ (sec)	3,920	8,280	15,500	20,200	29,300	36,700
$\overline{V}$ (ft/sec)	0.765	0.737	0.710	0.728	0.628	0.594
$\overline{A}$ (sq ft)	314	326	338	330	382	404
σ_x (ft)	222	632	1,410	2,910	2,720	2,950
$\overline{t}^{\frac{1}{2}}$ ($sec^{\frac{1}{2}}$)	62.5	91.0	124	142	171	192
α_3	0.5	1.4	1.5	1.6	1.0	0.9
M′ (curies)	0.339	0.302	0.338	0.305	0.282	0.272
M′/M	0.899	0.801	0.897	0.809	0.748	0.721
C_{max} ($\mu c/ft^3$)	1.34	0.55	0.31	0.18	0.13	0.10
t_p (sec)	3,360	7,230	13,200	17,500	27,100	33,600
$\frac{M'}{C_{max}\,\overline{A}\sqrt{2\pi}}$	321	672	1,290	2,040	2,270	2,690
V_* (ft/sec)	0.18	0.16	0.15	0.16	0.16	0.13

Table 20 -- Time-Concentration Data, Test 1-60

[Discharge: 300 cubic feet per second; Tracer:0.450 curies of Au 198 1/; Time of injection: 11:08.0 to 11:08.6 a.m. EST]

Section 1 X = 630 ft		Section 2 X = 3,310 ft		Section 3 X = 5,670 ft	
Time	Concentration	Time	Concentration	Time	Concentration
11:11.5 a.m.	0	11:25.0 a.m.	0	11:38.0 a.m.	0
11:12.0	2.00	11:26.0	0.15	11:39.0	0.12
11:12.5	16.50	11:27.0	1.13	11:40.0	.30
11:13.0	13.45	11:28.0	2.30	11:43.0	1.21
11:13.5	7.26	11:28.5	2.74	11:45.0	1.61
11:14.0	5.29	11:29.0	2.91	11:47.0	1.64
11:15.0	3.37	11:29.5	2.91	11:49.0	1.56
11:16.0	2.29	11:30.0	2.80	11:53.0	1.26
11:17.0	1.54	11:31.0	2.59	11:58.0	.86
11:18.0	1.03	11:33.0	2.18	12.03.0 p.m.	.53
11:20.0	.40	11:37.0	1.34	12:08.0	.30
11:24.0	.10	11:43.0	.60	12:13.0	.17
11:28.0	.04	11:49.0	.23	12:18.0	.10
11:33.0	.02	11:58.0	.08	12:28.0	.04
11:38.0	0	12:08.0 p.m.	.03	12:38.0	.01
		12:18.0	0	12:48.0	0

Section 4 X = 7,870 ft		Section 5 X = 11,000 ft		Section 6 X = 13,550 ft	
11:49.0 a.m.		12:10.0 p.m.		12:26.0 p.m.	
11:52.0	0.26	12:15.0	0.05	12:31.0	0.07
11:55.0	.67	12:20.0	0.25	12:36.0	.22
11:58.0	.95	12:25.0	.52	12:41.0	.40
12:00.0 m.	1.09	12:28.0	.64	12:45.0	.50
12:02.0 p.m.	1.13	12:31.0	.70	12:49.0	.58
12:04.0	1.10	12:34.0	.72	12:51.0	.59
12:06.0	1.04	12:37.0	.71	12:53.0	.59
12:08.0	.95	12:40.0	.65	12:57.0	.54
12:13.0	.72	12:44.0	.55	1:04.0	.44
12:18.0	.50	12:48.0	.45	1:13.0	.27
12:23.0	.31	12:58.0	.24	1:23.0	.14
12:28.0	.21	1:08.0	.12	1:33.0	.06
12:38.0	.08	1:18.0	.06	1:43.0	.03
12:48.0	.02	1:33.0	.03	2:03.0	.02
1:00.0		1:53.0		2:23.0	

1/ Concentrations are shown in micro-curies per cubic foot of Au 198.

Table 21 Channel Geometry and Flow Data, Test 1-60

Section	1	2	3	4	5	6
X (ft)	630	3,310	5,670	7,870	11,000	13,550
Q (cfs)[1]	249	276	280	269	286	308
V (ft/sec)[1]	1.65	1.82	1.88	1.74	1.64	1.49
A (sq ft)[1]	151	153	149	155	174	207
b (ft)[1]	46	63	57	58	65	70
d (ft)[1]	3.28	2.43	2.61	2.67	2.68	2.96
R (ft)[1]	3.07	2.41	2.56	2.61	2.62	2.91
T (^{o}F)	50	50	50	50	51	50
F (ft)	0.62	4.42	7.51	10.70	13.86	17.34
$S^{\frac{1}{2}}$	0.031	0.037	0.036	0.037	0.036	0.036
n	0.05	0.05	0.05	0.05	0.05	0.06

[1] Based on discharge measurements made one day before tracer injection. Other data obtained from observations made during tracer test.

Table 22 Analysis Data, Test 1-60

Q = 300 cfs; M = 0.045 curies

Section	1	2	3	4	5	6
$\overline{X}$ (ft)	630	3,310	5,670	7,870	11,000	13,550
$\overline{t}$ (sec)	380	1,640	2,740	3,650	5,630	6,720
$\overline{V}$ (ft/sec)	1.66	2.02	2.07	2.16	1.95	2.02
$\overline{A}$ (sq ft)	181	149	145	139	154	149
σ_x (ft)	73	780	1,190	1,550	1,600	2,010
$\overline{t}^{\frac{1}{2}}$ ($sec^{\frac{1}{2}}$)	19.5	40.5	52.4	60.4	74.4	82.0
α_3	1.5	1.7	1.4	1.3	0.8	1.1
M′ (curies)	0.616	0.596	0.560	0.494	0.439	0.394
M′/M	1.37	1.32	1.24	1.10	0.975	0.875
C_{max} ($\mu c/ft^3$)	16.5	2.91	1.64	1.13	0.72	0.59
t_p (sec)	270	1,290	2,340	3,240	5,160	6,180
$\frac{M'}{C_{max}\,\overline{A}\sqrt{2\pi}}$	82	550	939	1,260	1,580	1,820
V_* (ft/sec)	0.31	0.33	0.33	0.34	0.33	0.35

Table 23 -- Time-Concentration Data, Test 2-60

[Discharge: 3,000 cubic feet per second; Tracer: 3.770 curies of Au 198 1/; Time of injection: 10:17.0 to 10:18.0 a.m. EST]

Section 1 X = 2,260 ft		Section 2 X = 5,170 ft		Section 3 X = 8,170 ft	
Time	Concentration	Time	Concentration	Time	Concentration
10:25.5 a.m.	0	10:37 a.m.	0	10:52.0 a.m.	0
10:26.0	0.78	10:38.0	0.50	10:53.0	0.51
10:26.5	5.27	10:39.0	2.42	10:54.0	2.06
10:27.0	7.70	10:40.0	4.13	10:55.0	4.28
10:27.5	6.74	10:40.5	4.46	10:56.0	4.66
10:28.0	4.07	10:41.0	4.26	10:57.0	4.17
10:29.0	1.83	10:42.0	3.45	10:58.0	3.45
10:30.0	.89	10:44.0	1.96	11:00.0	2.08
10:32.0	.32	10:48.0	.69	11:04.0	.88
10:34.0	.17	10:52.0	.26	11:08.0	.36
10:36.0	.10	10:58.0	.12	11:14.0	.20
10:38.0	.05	11:04.0	.08	11:20.0	.10
10:43.0	.03	11:10.0	.06	11:30.0	.05
10:48.0	.01	11:20.0	.02	11:40.0 a.m.	.02
10:53.0	0	11:40.0	0	12:00.0 m	0

Section 4 X = 11,800 ft		Section 5 X= 15,300 ft		Section 6 X = 19,300 ft	
11:07.0 a.m.	0	11:28.0 a.m.	0	11:47.0 a.m.	0
11:08.0	0.11	11:30.0	0.24	11:50.0	0.06
11:10.0	1.20	11:32.0	.94	11:53.0	.49
11:12.0	2.50	11:34.0	1.46	11:56.0	1.10
11:12.5	2.60	11:35.0	1.47	11:58.0	1.21
11:13.0	2.54	11:36.0	1.44	12:00.0 m,	1.10
11:15.0	1.78	11:38.0	1.12	12:03.0 p.m.	.82
11:17.0	1.19	11:40.0	.82	12:06.0	.66
11:21.0	.61	11:45.0	.46	12:12.0	.45
11:25.0	.37	11:50.0	.31	12:20.0	.32
11:30.0	.23	12:00.0 m	.18	12:30.0	.22
11:35.0	.15	12:10.0 p.m.	.10	12:40.0	.15
11:45.0	.08	12:20.0	.05	1:00.0	.07
12:00.0 m,	.04	12:30.0	.02	1:20.0	.04
12:20.0 p.m.	0	12:50.0	0	1:40.0	0

1/ Concentrations are shown in micro-curies per cubic foot of Au 198.

Table 24 Channel Geometry and Flow Data, Test 2-60

Section	1	2	3	4	5	6
X (ft)	2,260	5,170	8,170	11,800	15,300	19,300
Q (cfs)[1]	3,700	3,740	3,690	3,890	3,680	3,600
V (ft/sec)[1]	2.96	3.40	3.10	2.61	2.49	2.28
A (sq ft)[1]	1,250	1,100	1,190	1,490	1,480	1,580
b (ft)[1]	204	210	185	195	204	171
d (ft)[1]	6.13	5.24	6.43	7.64	7.25	9.24
R (ft)[1]	6.01	5.19	6.38	7.48	7.15	9.10
T (°F)	41	43	41	41	42	41
F (ft)	2.10	3.22	4.27	5.05	6.41	7.38
$S^{\frac{1}{2}}$	0.030	0.025	0.023	0.021	0.020	0.020
n	0.06	0.05	0.05	0.05	0.05	0.05

[1] Based on discharge measurements made one day before tracer injection. Other data obtained from observations made during tracer test.

Table 25 Analysis Data, Test 2-60

Q = 3,000 cfs; M = 3.77 curies

Section	1-C	2	3	4	5	6
$\bar{X}$ (ft)	2,260	5,170	8,170	11,800	15,300	19,300
$\bar{t}$ (sec)	678	1,640	2,600	3,730	5,210	7,020
$\bar{V}$ (ft/sec)	3.33	3.15	3.14	3.16	2.94	2.75
$\bar{A}$ (sq ft)	901	952	955	949	1,020	1,090
σ_{x_1} (ft)	180	433	529	568	766	1,010
$\bar{t}^{\frac{1}{2}}$ ($sec^{\frac{1}{2}}$)	26.0	40.5	51.0	61.1	72.2	83.8
α_3	1.2	1.3	1.2	1.1	1.0	1.0
M′ (curies)	3.25	5.14	6.34	4.56	3.87	4.98
M′/M	0.862	1.36	1.68	1.21	1.03	1.32
C_{max} ($\mu c/ft^3$)	7.70	4.46	4.66	2.60	1.47	1.21
t_p (sec)	600	1,410	2,340	3,330	4,680	6,060
$\frac{M'}{C_{max}} \frac{1}{\bar{A}\sqrt{2\pi}}$	187	482	568	736	1,030	1,508
V_* (ft/sec)	0.42	0.32	0.33	0.34	0.30	0.34

Table 26 -- Time-Concentration Data, Test 3-60

[Discharge: 900 cubic feet per second; Tracer: 1.58 curies of Au^{198} 1/; Time of injection: 11:01.0 to 11:02.0 a.m. PDT]

Section 1 X = 1,000 ft		Section 2 X = 3,000 ft		Section 3 X = 6,000 ft	
Time	Concentration	Time	Concentration	Time	Concentration
11:07.3 a.m.	0	11:19.9 a.m.	0	11:40.0 a.m.	0
11:07.5	0.40	11:20.5	1.48	11:41.0	0.32
11:07.7	1.15	11:21.0	4.79	11:42.0	2.10
11:07.9	14.50	11:21.5	9.73	11:43.0	4.96
11:08.1	24.46	11:22.0	14.06	11:44.0	8.64
11:08.2	24.84	11:22.2	14.78	11:44.4	9.20
11:08.3	24.78	11:22.5	14.29	11:44.8	9.02
11:08.5	23.60	11:23.0	11.36	11:45.2	8.50
11:08.7	16.26	11:23.5	6.20	11:46.0	5.94
11:08.9	8.70	11:24.0	3.45	11:47.0	3.42
11:09.1	5.60	11:24.5	1.68	11:48.0	1.81
11:09.3	3.76	11:25.0	.76	11:49.0	.83
11:09.5	2.46	11:26.0	.22	11:51.0	.24
11:09.9	.64	11:27.0	.07	11:53.0	.08
11:10.3	0	11:28.0	0	11:55.0	0

Section 4 X = 9,000 ft		Section 5 X = 13,000 ft	Section 6 X = 18,000 ft	
11:59.5 a.m.	0	Detector did not operate	1:00.0 p.m.	0
12:01.0 p.m.	0.61		1:03.0	0.07
12:02.0	1.46		1:06.0	.37
12:03.0	3.34		1:09.0	1.58
12:04.0	5.32		1:11.0	2.04
12:04.5	5.80		1:13.0	1.86
12:05.0	5.68		1:16.0	1.22
12:06.0	4.66		1:19.0	.82
12:07.0	3.32		1:23.0	.47
12:08.0	2.04		1:27.0	.27
12:10.0	.85		1:31.0	.14
12:12.0	.54		1:35.0	.08
12:14.0	.33		1:39.0	.05
12:18.0	.14		1:43.0	.02
12:22.0	0		1:47.0	0

1/ Concentrations are shown in micro-curies per cubic foot of Au 198.

Table 27 Channel Geometry and Flow Data, Test 3-60

Section	1	2	3	4	5	6
X (ft)	1,000	3,000	6,000	9,000	13,000	18,000
Q (cfs)[1]	911	897	885	900	901	903
V (ft/sec)[1]	2.20	2.19	2.33	2.17	2.00	2.32
A (sq ft)[1]	414	410	379	415	450	390
b (ft)[1]	80	78	80	82	89	72
d (ft)[1]	5.18	5.26	4.74	5.06	5.06	5.42
R (ft)[1]	4.88	5.02	4.55	4.87	4.85	5.10
T (^{o}F)			Not observed			
F (ft)	0.12	0.37	0.76	0.97	-	2.01
$S^{\frac{1}{2}}$	0.011	0.011	0.011	0.010	-	0.011
n	0.02	0.02	0.02	0.02	-	0.02

[1] Based on discharge measurements made one day before tracer injection. Other data obtained from observations made during tracer test.

Table 28 Analysis Data, Test 3-60

Q = 900 cfs; M = 1.58 curies

Section	1-C	2	3	4	5	6
X (ft)	1,000	3,000	6,000	9,000	13,000	18,000
$\overline{t}$ (sec)	447	1,290	2,640	3,900	Probe inoperative	8,040
$\overline{V}$ (ft/sec)	2.24	2.33	2.27	2.31		2.24
$\overline{A}$ (sq ft)	402	386	396	390		402
σ_x (ft)	72.8	144	224	331		640
$\overline{t}^{\frac{1}{2}}$ ($sec^{\frac{1}{2}}$)	21.1	35.9	51.4	62.4		89.7
α_3	1.3	0.9	0.9	1.3		1.2
M′ (curies)	1.39	1.87	2.07	1.73		1.33
M′/M	0.880	1.18	1.31	1.09		0.842
C_{max} ($\mu c/ft^3$)	24.84	14.78	9.20	5.80		2.04
t_p (sec)	432	1,270	2,600	3,810		7,800
$\frac{M'}{C_{max}} \frac{1}{\overline{A}\sqrt{2\pi}}$	55.4	131	227	305		646
V_* (ft/sec)	0.14	0.14	0.13	0.12		0.14

Table 29 -- Concentration Data, Test 4-60

[Discharge: 950 cubic feet per second; Tracer: 1.21 curies of Au 198 1/; Time of injection: 9:06.0 to 9:07.0 a.m. PDT]

Section 1 X = 1,000 ft		Section 2 X =3,000 ft		Section 3 X = 9,000 ft	
Time	Concentration	Time	Concentration	Time	Concentration
9.11.3 a.m.	0	9.24.2 a.m.	0	9:59.0 a.m.	0
9:11.6	2.90	9:24.6	0.27	10:01.0	0.02
9:11.9	10.05	9:25.0	1.10	10:03.0	0.04
9:12.2	16.50	9:25.5	3.25	10:05.0	0.10
9:12.5	20.83	9:26.0	7.10	10:07.0	1.00
9:12.8	19.96	9:26.5	8.06	10:09.0	3.52
9:13.0	15.71	9:27.0	7.52	10:09.5	3.86
9:13.5	6.14	9:27.5	4.80	10:10.0	3.80
9:14.0	2.68	9:28.0	2.91	10:12.0	2.34
9:14.5	1.49	9:29.0	.95	10:14.0	1.10
9:15.0	.97	9:30.0	.25	10:18.0	.42
9:16.0	.41	9:32.0	.08	10:22.0	.18
9:17.0	.16	9:34.0	.05	10:26.0	.10
9:18.0	.07	9:38.0	.02	10:30.0	.04
9:19.0	0	9:42.0	0	10.34.0	0

Section 4 X = 13,000 ft		Section 5 X = 18,000 ft		Section 6 X = 63,750 ft	
10:31.0 a.m.	0	11:05.0 a.m.	0	4:03.0 p.m.	0
10:33.0	0.05	11:07.0	0.04	4:10.0	0.06
10:35.0	.46	11:09.0	.17	4:17.0	.21
10:37.0	1.59	11:11.0	.57	4:24.0	.41
10:39.0	2.37	11:13.0	1.03	4:31.0	.50
10:41.0	2.00	11:15.0	1.25	4:33.5	.52
10:43.0	1.29	11:17.0	1.15	4:36.0	.50
10:45.0	.85	11:19.0	.92	4:43.0	.42
10:47.0	.55	11:21.0	.71	4:50.0	.32
10:49.0	.39	11:23.0	.55	4:57.0	.22
10:51.0	.27	11:25.0	.43	5:04.0	.13
10:55.0	.13	11:29.0	.26	5:11.0	.08
10:59.0	.07	11:35.0	.11	5:18.0	.04
11:03.0	.03	11:41.0	.05	5:25.0	.02
11:10.0	0	11:47.0	0	5:35.0	0

1/ Concentrations are shown in micro-curies per cubic foot of Au 198.

Table 30 Channel Geometry and Flow Data, Test 4-60

Section	1	2	3	4	5	6
X (ft)	1,000	3,000	6,000	9,000	13,000	18,000
Q (cfs)[1]	911	897	885	900	901	903
V (ft/sec)[1]	2.20	2.19	2.33	2.17	2.00	2.32
A (sq ft)[1]	414	410	379	415	450	390
b (ft)[1]	80	78	80	82	89	72
d (ft)[1]	5.18	5.26	4.74	5.06	5.06	5.42
R (ft)[1]	4.88	5.02	4.55	4.87	4.85	5.10
T (°F)			Not observed			
F (ft)	0.12	0.37	0.76	0.97	1.47	2.01
$S^{\frac{1}{2}}$	0.011	0.011	0.011	0.010	0.011	0.011
n	0.02	0.02	0.02	0.02	0.02	0.02

[1] Based on discharge measurements made two days before tracer injection. Other data obtained from observations made during tracer test.

Table 31 Analysis Data; Test 4-60

Q = 950 cfs; M = 1.21 curies

Section	1-C	2	3	4	5	6
$\overline{X}$ (ft)	1,000	3,000	9,000	13,000	18,000	63,750
$\overline{t}$ (sec)	411	1,260	3,940	5,760	7,980	27,200
$\overline{V}$ (ft/sec)	2.43	2.38	2.28	2.26	2.26	2.34
$\overline{A}$ (sq ft)	391	399	417	420	420	406
σ_x (ft)	119	138	340	474	728	2,210
$\overline{t^{\frac{1}{2}}}$ ($sec^{\frac{1}{2}}$)	20.3	35.5	62.8	75.9	89.3	165
α_3	0.9	0.7	1.2	1.2	1.2	0.6
M′ (curies)	1.83	1.13	1.39	1.19	0.931	1.11
M′/M	1.51	0.934	1.15	0.983	0.769	0.917
C_{max} ($\mu c/ft^3$)	20.83	8.06	3.86	2.37	1.25	0.52
t_p (sec)	390	1,230	3,810	5,580	7,740	26,800
$\frac{M'}{C_{max}\,\overline{A}\sqrt{2\pi}}$	89.8	140	344	477	708	2,090
V_* (ft/sec)	0.14	0.14	0.13	0.14	0.14	-

Table 32 -- Time-Concentration Data, Test 1-61

[Discharge: 1800 cubic feet per second; Tracer: 2.45 curies of Au 198 1/; Time of injection: 10:29.0 to 10:30.0 a.m. EST]

Section 1-C X = 2,260 ft		Section 2 X = 5,170 ft		Section 3 X = 8,170 ft	
Time	Concentration	Time	Concentration	Time	Concentration
10:37.0 a.m.	0	10:51.0 a.m.	0	11:09.0 a.m.	0
10:38.0	1.02	10:52.0	0.21	11:10.0	0.12
10:38.4	5.40	10:53.0	1.00	11:11.0	.38
10:38.8	9.70	10:54.0	3.28	11:12.0	1.17
10:39.1	11.30	10:55.0	4.93	11:13.0	2.40
10:39.4	10.80	10:55.5	5.28	11:14.2	3.32
10:39.8	8.42	10:56.0	5.11	11:15.0	3.20
10:40.2	6.10	10:57.0	3.83	11:16.0	2.76
10:40.6	4.35	10:58.0	2.48	11:18.0	1.76
10:41.0	2.76	11:00.0	1.29	11:20.0	1.04
10:42.0	1.35	11:02.0	.73	11:23.0	.65
10:43.0	.90	11:04.0	.47	11:26.0	.43
10:45.0	.50	11:06.0	.34	11:30.0	.27
10:48.0	.25	11:10.0	.19	11:40.0	.11
10:51.0	.10	11:15.0	.09	11:55.0	.05
10:55.0	0	11:20.0	0	12:15.0	0

Section 4 X = 11,800 ft		Section 5 X = 15,300 ft		Section 6 X = 19,300 ft	
11:30.0 a.m.	0	11:43.0 a.m.	0	12:24.0	0
11:32.0	0.12	11:46.0	0.17	12:27.0	0.09
11:34.0	1.05	11:48.0	.43	12:30.0	.40
11:36.0	2.22	11:50.0	1.35	12:33.0	.76
11:37.0	2.40	11:52.0	1.60	12:35.0	.86
11:38.0	2.31	11:54.0	1.43	12:37.0	.82
11:40.0	1.60	11:56.0	1.11	12:40.0	.69
11:42.0	1.15	11:59.0	.78	12:45.0	.50
11:46.0	.68	12:04.0 p.m.	.50	12:50.0	.38
11:50.0	.42	12:09.0	.38	1:00.0	.27
11:54.0	.29	12:19.0	.24	1:15.0	.18
11:59.0	.21	12:29.0	.15	1:30.0	.12
12:09.0 p.m.	.12	12:44.0	.07	1:50.0	.07
12:29.0	.05	12:59.0	.04	2:15.0	.03
12:50.0	0	1:25.0	0	2:45.0	0

1/ Concentrations are shown in micro-curies per cubic foot of Au 198.

Table 33 Channel Geometry and Flow Data, Test 1-61

Section	1	2	3	4	5	6
X (ft)	2,260	5,170	8,170	11,800	15,300	19,300
Q (cfs)[1]	3,030	2,820	3,150	3,070	2,960	3,010
V (ft/sec)[1]	2.66	3.22	3.03	2.26	2.29	2.03
A (sq ft)[1]	1,140	876	1,040	1,360	1,290	1,480
b (ft)[1]	200	165	160	183	175	166
d (ft)[1]	5.70	5.31	6.50	7.43	7.37	8.92
R (ft)[1]	5.56	5.25	6.41	7.21	7.21	8.74
T (°F)	67	67	67	68	68	68
F (ft)	2.30	4.12	4.66	5.32	6.49	7.35
$S^{\frac{1}{2}}$	0.032	0.028	0.024	0.021	0.021	0.020
n	0.08	0.08	0.08	0.08	0.08	0.08

[1] Based on discharge measurements made one day before tracer injection. Other data obtained from observations made during tracer test.

Table 34 Analysis Data, Test 1-61

Q = 1,800 cfs; M = 2.45 curies

Section	1-C	2	3	4	5	6
$\bar{X}$ (ft)	2,260	5,170	8,170	11,800	15,300	19,300
$\bar{t}$ (sec)	684	1,730	3,070	4,570	5,740	8,940
$\bar{V}$ (ft/sec)	3.30	2.99	2.66	2.58	2.67	2.16
$\bar{A}$ (sq ft)	545	602	677	698	674	833
σ_x (ft)	188	330	558	544	830	1,390
$\overline{t^{\frac{1}{2}}}$ ($sec^{\frac{1}{2}}$)	26.2	41.6	55.4	67.6	75.8	94.6
α_3	1.2	0.7	1.5	1.0	1.4	1.6
M′ (curies)	3.02	3.19	3.06	3.05	2.96	2.79
M′/M	1.23	1.30	1.25	1.24	1.21	1.14
C_{max} ($\mu c/ft^3$)	11.30	5.28	3.32	2.40	1.60	0.86
t_p (sec)	606	1,590	2,710	4,080	4,980	7,560
$\frac{M'}{C_{max}} \frac{1}{\bar{A}\sqrt{2\pi}}$	195	400	542	726	1,090	1,550
V_* (ft/sec)	0.43	0.36	0.34	0.32	0.32	0.34

Table 35 -- Time-Concentration Data Test 2-61

[Discharge: 48.0 cubic feet per second; Tracer: 0.112 curies of Au 198 1/; Time of injection: 9:02.0 to 9:03.0 a.m. EDT]

Section 1 X = 630 ft		Section 2 X = 3,310 ft		Section 3 X = 5,670 ft	
Time	Concentration	Time	Concentration	Time	Concentration
9:08.4 a.m.	0	9:42.0 a.m.	0	10:10.0 a.m.	0
9:08.8	0.56	9:45.0	0.10	10:15.0	0.23
9:09.2	1.56	9:48.0	.55	10:20.0	.54
9:09.6	4.13	9:51.0	.96	10:25.0	.73
9:10.0	7.68	9:54.0	1.09	10:28.0	.78
9:10.4	9.54	9:56.5	1.12	10:31.5	.80
9:10.6	9.69	9:59.0	1.07	10:35.0	.77
9:10.8	9.54	10:02.0	.97	10:40.0	.68
9:11.2	8.27	10:06.0	.82	10:50.0	.47
9:12.0	5.30	10:10.0	.64	11:00.0	.30
9:13.0	2.91	10:20.0	.36	11:20.0	.13
9:15.0	1.58	10:40.0	.15	11:40.0 a.m.	.07
9:17.0	1.04	11:00.0	.08	12:00.0 m	.04
9:22.0	.39	11:20.0	.04	12:30.0 p.m.	.02
9:27.0	0	11:52.0	0	1:00.0	0

Section 4 X = 7,870 ft		Section 5 X =11,000 ft		Section 6 X = 13,550 ft	
10:35.0 a.m.	0	11:37.0	0	12:30.0 p.m.	0
10:45.0	0.21	11:43.0	0.04	12:40.0	0.07
10:50.0	.39	11:53.0 a.m.	.13	12:50.0	.17
10:55.0	.52	12:03.0 p.m.	.23	1:00.0	.23
11:00.0	.59	12:13.0	.31	1:10.0	.27
11:05.0	.62	12:18.0	.33	1:15.0	.28
11:10.0	.60	12:23.0	.34	1:20.0	.28
11:20.0	.49	12:28.0	.34	1:25.0	.28
11:30.0	.37	12:33.0	.33	1:30.0	.27
11:50.0 a.m.	.18	12:50.0	.26	1:40.0	.24
12:10.0 p.m.	.10	1:10.0	.16	2:00.0	.18
12:30.0	.06	1:30.0	.10	2:30.0	.10
1:00.0	.03	2:00.0	.06	3:10.0	.04
1:30.0	.01	2:50.0	.03	4:00.0	.02
2:00.0	0	3:50.0	0	5:00.0	0

1/ Concentrations are shown in micro-curies per cubic foot of Au 198.

Table 36 Channel Geometry and Flow Data, Test 2-61

Section	1	2	3	4	5	6
X (ft)	630	3,310	5,670	7,870	11,000	13,550
Q (cfs)[1]	63.3	63.8	63.6	67.6	68.6	68.7
V (ft/sec)[1]	0.64	1.05	0.79	0.89	0.71	0.79
A (sq ft)[1]	99.4	61.0	80.5	75.7	96.6	86.5
b (ft)[1]	44	51	57	49	60	54
d (ft)[1]	2.26	1.20	1.41	1.54	1.61	1.60
R (ft)[1]	2.18	1.18	1.39	1.50	1.59	1.59
T (°F)	71	70	70	71	72	72
F (ft)	0.73	4.86	7.89	11.13	14.02	17.60
$S^{\frac{1}{2}}$	0.034	0.038	0.037	0.038	0.036	0.036
n	0.18	0.13	0.12	0.12	0.13	0.13

[1] Based on discharge measurements made one day before tracer injection. Other data obtained from observations made during tracer test.

Table 37 Analysis Data, Test 2-61

Q = 48 cfs; M = 0.112 curies

Section	1	2	3	4	5	6
$\overline{X}$ (ft)	630	3,310	5,670	7,870	11,000	13,550
$\overline{t}$ (sec)	642	4,150	6,360	8,580	13,700	17,100
$\overline{V}$ (ft/sec)	0.981	0.798	0.892	0.917	0.803	0.792
$\overline{A}$ (sq ft)	48.9	60.2	53.8	52.3	59.8	60.6
σ_x (ft)	68.9	604	899	1,300	1,790	2,010
$\overline{t}^{\frac{1}{2}}$ ($sec^{\frac{1}{2}}$)	25.3	64.4	79.7	92.6	117	131
α_3	1.0	1.2	0.9	1.1	1.2	1.0
M′ (curies)	0.104	0.103	0.102	0.102	0.085	0.079
M′/M	0.929	0.920	0.911	0.911	0.759	0.705
C_{max} ($\mu c/ft^3$)	9.69	1.12	0.80	0.62	0.34	0.28
t_p (sec)	516	3,270	5,370	7,380	12,100	15,500
$\frac{M'}{C_{max}\,\overline{A}\sqrt{2\pi}}$	87.0	609	948	1,260	1,670	1,860
V_* (ft/sec)	0.29	0.24	0.25	0.26	0.26	0.26

An effort was made to conduct the tests on recession so that steady-state conditions could be closely approximated. This condition was not always fulfilled as shown in Table 37.

Table 37. -Change in discharge

None of the channel geometry and flow data were used directly in the dispersion analysis. However, such data do characterize the study reaches and will be useful in subsequent analyses when more appropriate models are developed.

Table 37. - Change in discharge

	Discharge (cfs)		
Test	Prior day	Day of test	Percent change
1-59	57.3	54.3	-6
2-59	359	323	-11
3-59	36.0	35.0	-3
4-59	146	140	-4
5-59	197	240	+21
1-60	278	300	+7
2-60	3720	3000	-19
3-60	899	900	0
4-60	899	950	+6
1-61	2990	1800	-40
2-61	65.9	48.0	-27

Selected References

Archibald, R. S., 1950, Radioactive tracers in flow tests, Jour., Boston Soc. Civ. Eng. 37, 49-116.

Einstein, A., 1905, Uber die von der molekular-kinetischen theorie der Warme geforderte Bewegung von in ruhenden Flussigkeiten suspendierten teilchen, Ann. Physik v. 17, p. 549-560.

Elder, J. W., 1959, The dispersion of a marked fluid in turbulent shear flow, Jour. Fluid Mech., v. 5, no. 4, p. 544-560.

Ellis, W. R., et al, 1958, The use of a radioactive tracer (Iodine 131) in the investigation of a power station cooling pond at Maitland, N.S.W., Australian Atomic Energy Comm., AAEC/E.8.

Frederick, B. J. and Godfrey, R. G., 1961, The effect of finite boundaries on measurement of Gold-198 with a scintillation detector, Prof. Paper 424-D.

Glover, R. W., 1962, Dispersion of dissolved materials in flowing streams, Prof. Paper 433B.

Godfrey, R. G., 1961, Observation of unsteady phenomena in an open channel, Prof. Paper 424-C.

Hull, D. E. and Kent, J. W., 1952, Radioactive tracers to mark interfaces and measure intermixing in pipelines, Industr. Engr. Chem., v. 44, Part 2, no. 11, p. 2745-2750.

Hull, D. E. and Macomber, M., 1958, Flow Measurements by the total count method, Proc. 2nd U.N. Int. Conf. on the Peacefull Uses of Atomic Energy, 19, 324-332.

Parker, F. L., 1958, Radioactive tracers in hydrologic studies, Amer. Geophs. Union, v. 39, no. 3, p. 434-439.

Price, W. J., 1958, Nuclear radiation detection, McGraw-Hill Book Co., Inc., New York, N. Y.

Simpson, E. S., Beetem, W. A. and Ruggles, F. H., 1958, Radiotracer experiments in the Mohawk River, New York, to study sewage path and dilution, Amer. Geophs. Union, v. 39, p. 427-433.

Taylor, G. I., 1954, Dispersion of matter in turbulent flow through a pipe, Royal Soc. London Proc., A-223, p. 446-468.

Tracy, H. J. and Lester, C. M., 1961, Resistance coefficients and velocity distribution smooth rectangular channel, Water Supply Paper 1592-A.

United States National Bureau of Standards, 1959, Maximum permissable body burdens and maximum permissable concentrations of radionuclides in air and in water for occupational exposure, Handbook 69.